

國立臺灣大學工程學院化學工程學系

碩士論文

Department of Chemical Engineering

College of Engineering


National Taiwan University

Master Thesis

最佳化批次結晶程序之目標函數選擇

Comparison of objective functions for seeded batch

crystallization



許哲維

Che-Wei Hsu

指導教授：吳哲夫 博士

Advisors: Jeffrey D. Ward, Ph.D.

中華民國 100 年 7 月

July, 2011

## 致謝

首先在此由衷的感謝吳哲夫教授這兩年的付出，特別是在余政靖教授剛過世時，實驗室一片混亂的情況下接下了團隊並指導。另外也感謝陳誠亮教授、錢義隆教授、黃孝平教授與蕭立鼎教授對於研究的指導。

在這兩年的研究期間，感謝同屆的朋友(雨利、冠安、承勳、翊軒、信杰、少儂)在修課和研究之餘的陪伴。感謝實驗室曾經指導過我的學長姐(愛真、建凱、乾元、玉龍、愷悌、雅玲)和同實驗室的同事們(郁迪、傳真、均彥、孟達、育賢、鎮宇、宗翰)，最後感謝實驗室的學弟妹(偉倫、紹群、騰雲)。



## 緒論

結晶是一個常被用來作為液態固態分離的程序。而一個結晶槽的成品可以用結晶大小分佈函數(Crystal Size Distribution Function, CSD)來描述。成品的好壞將影響下游程序的效率，例如過濾或是乾燥程序。在結晶的過程中，同時會出現結晶成核(crystal nucleation)與結晶成長(crystal growth)現象，在大多數的情況下結晶成核現象是不受歡迎的。一個控制得好的結晶槽，可以有效抑制結晶成核現象的發生。

要最佳化一個結晶程序可以從兩方面來著手，一種是改善晶種的性質，另一種是改善冷卻的方法。而不管是使用哪一種手段，都需要一個目標函數來評斷結果的好壞。在這個研究中，我們比較前人在這個領域上使用過的目標函數，希望能夠發現一個最適合的目標函數。

在使用各個目標函數後，我們發現有些目標函數的結果藉由產生大量的成核現象以達到其目標函數值的最小值。但以一個先加入晶種的結晶程序而言，其目標是將晶種長大並避免成核現象的發生，前述達到其目標函數值的方法是與其牴觸的。事實上在真實的程序裡，在結晶之後很有可能經過一個過濾的程序將過小的晶體或是新成核的晶體移除。所以對於各個不同的目標函數，我們除了直接比較用其最佳化的結果的目標函數值以外，也比較新成核晶體被移除後的目标函數值。最後我們發現使用目標函數”最小化新成核晶體的

質量”來最佳化，其結果在新成核晶體被移除後，對於各個目標函數值都有較佳的值。

對於目標函數”最小化結晶分佈函數的變異係數”，我們發現與其最佳化結晶成長曲線，使用晶種性質作為控制變數有較佳的效果。較大量的晶種質量與較集中的晶種分佈，在使用”最小化結晶分佈函數的變異係數”作為目標函數時，將有效防止大量成核現象的發生。

最後，我們探討結晶成核速率式中，在晶體體積項(Third Moment)較高的幕次對於最佳化程序的影響。我們發現，較高的幕次將抑制成核現象的發生，造成最佳化的結果有較佳的表現。另外較高的幕次也將使得最佳化晶體成長曲線在程序的一開始有較高的值。



## Abstract

Crystallization is a widely used process for liquid solid separation. The products from this process are crystals, which can be described by a distribution function called “crystal size distribution function (CSD)”. The properties of the crystals affect the efficiency of downstream process, such as filtration or drying. During the process both crystal nucleation and crystal growth happens, and most of the time, the crystal nucleation is undesirable. A well-controlled crystallizer can produce crystals with less crystal nucleation.

Researchers have optimize a crystallization processes by improving the seed properties or the cooling policy. In both cases an objective function is required. In this work we compare the objective function that researchers have used, to see which objective function is best when optimizing the cooling policy for a batch crystallizer.

The result shows that some of the objective functions are minimized by producing a large amount of nuclei. However, for a seeded batch crystallizer the idea is to grow the seed crystals while suppressing the nucleation. Moreover, in industrial practice, the product crystals would probably be filtered so that fines (nucleated crystals) would be removed. Therefore, for each objective function we also determine the objective value after the

nucleated crystals are removed, to see whether the result from each objective function is still the best. After the analysis we conclude that the objective function “minimizing the nucleated crystal mass” is better than others.

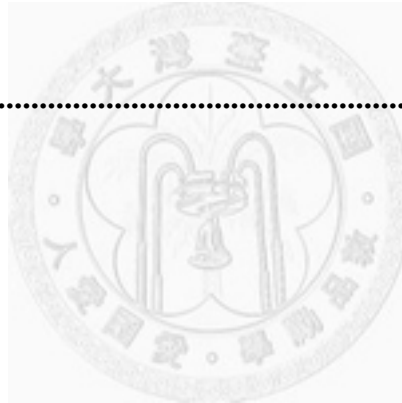
In this work we also discuss the utility of changing seed properties when using “minimizing weight coefficient of variation” as objective function. We found that if the seed distribution is too wide, the system would be more likely to generate a narrow distribution crystal by excess nucleation. To prevent excess nucleation and achieve a narrow product CSD, a large seed loading and a narrow seed distribution helps.

Finally, we also considered the effect of using different nucleation parameters. We changed the exponent on third moment term in nucleation rate equation. The result shows that for higher value of the exponent, the nucleation rate is suppressed, and the performance is better when the growth rate trajectory is optimized using the objective function “minimizing nucleated crystal mass.” The optimized result also mention that for higher value of the exponent on third moment term in nucleation rate equation, higher growth at the beginning of the batch is desirable.

# Table Of Content

List Of Figures.....	viii
List Of Tables .....	xii
1. Introduction .....	1
1.1. Overview.....	1
1.2. Literature Survey .....	4
2. Dimensionless Model.....	8
2.1. Dimensionless Moment Equations .....	8
2.2. Seed .....	12
3. Optimization by Simulated Annealing .....	15
1.1. Simulated Annealing .....	15
4.1. Control Variable .....	22
4.2. Final Mass Constraint.....	22
4. Discussion .....	24
4.1. Objective Function Classification .....	24
4.2. Comparison Method.....	27

<b>4.3. Weight COV and Number COV .....</b>	<b>29</b>
<b>4.5. Single Moment Objective Functions.....</b>	<b>44</b>
<b>4.6. Objective Function Category Comparison .....</b>	<b>51</b>
<b>4.7. Other Solution For Minimizing Coefficient of variation .....</b>	<b>57</b>
<b>4.8. The Effect of Changing j.....</b>	<b>63</b>
<b>5. Conclusion.....</b>	<b>73</b>
<b>6. Notations.....</b>	<b>75</b>
<b>7. Reference.....</b>	<b>77</b>





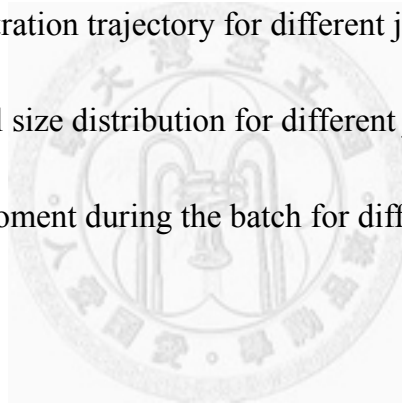
## List Of Figures

<b>Figure 1:</b> Supersaturation and metastable zone. [1] .....	2
<b>Figure 2:</b> The parabolic seed crystal size distribution (CSD) function. ....	12
<b>Figure 3:</b> Representation of optimization by simulated annealing. ....	17
<b>Figure 4:</b> The annealing temperature. ....	18
<b>Figure 5:</b> Simulation annealing algorithm. ....	21
<b>Figure 6:</b> Final crystal size distribution for different objectives. ....	29
<b>Figure 7:</b> The optimal growth trajectory using objective function, minimizing weight coefficient of variation and minimizing number coefficient of variation. ....	30
<b>Figure 8:</b> The optimal nucleation rate trajectory using objective function, minimizing weight coefficient of variation and minimizing number coefficient of variation. ....	31
<b>Figure 9:</b> Weight coefficient of variation and number coefficient of variation value for different objectives. ....	32
<b>Figure 10:</b> The optimal concentration trajectory using objective function, minimizing weight coefficient of variation and minimizing number coefficient of variation. ....	34

<b>Figure 11:</b> Different order of moment plot during the batch time for using objective function minimizing weight coefficient of variation and minimizing number coefficient of variation. ....	35
<b>Figure 12:</b> The optimal nucleation rate trajectory using objective function, minimizing weight mean size and minimizing number mean size. ....	36
<b>Figure 13:</b> The optimal growth trajectory using objective function, minimizing weight mean size and minimizing number mean size. ....	37
<b>Figure 14:</b> The optimal concentration trajectory using objective function, minimizing weight mean size and minimizing number mean size. ....	38
<b>Figure 15:</b> Different order of moment plot during the batch time for using objectives function minimizing weight mean size and minimizing number mean size. ....	40
<b>Figure 16:</b> Weight mean size and number mean size value for different objectives. ....	42
<b>Figure 17:</b> Final crystal size distribution for different objectives. ....	43
<b>Figure 18:</b> Nucleated crystal moments of for different objectives. ....	45
<b>Figure 19:</b> Seeded crystal moments for different objectives. ....	46
<b>Figure 20:</b> Final crystal size distribution for different objectives. ....	47

<b>Figure 21:</b> Different order of moments during the batch using minimizing $\mu_{n0}$ , $\mu_{n1}$ , $\mu_{n2}$ and $\mu_{n3}$ as objective function.....	49
<b>Figure 22:</b> The optimal nucleation rate trajectory using minimizing $\mu_{n0}$ , $\mu_{n1}$ , $\mu_{n2}$ and $\mu_{n3}$ as objective function. ....	50
<b>Figure 23:</b> The optimal growth rate trajectory using minimizing $\mu_{n0}$ , $\mu_{n1}$ , $\mu_{n2}$ and $\mu_{n3}$ as objective function. ....	50
<b>Figure 24:</b> The optimal growth trajectory using minimizing $\mu_{n3}$ , weight coefficient of variation and maximizing weight mean size. ....	52
<b>Figure 25:</b> The optimal nucleated trajectory using minimizing $\mu_{n3}$ , weight coefficient of variation and maximizing weight mean size. ....	52
<b>Figure 26:</b> The optimal concentration trajectory using minimizing $\mu_{n3}$ , weight coefficient of variation and maximizing weight mean size. ....	53
<b>Figure 27:</b> Different moments during the batch using minimizing $\mu_{n3}$ , weight coefficient of variation and maximizing weight mean size. ....	54
<b>Figure 28:</b> Weight mean size, weight coefficient of variation and third moment values for different objectives. ....	55
<b>Figure 29:</b> Final crystal size distribution for different objectives. ....	56
<b>Figure 30:</b> Initial crystal size distribution which is used for minimizing weight coefficient of variation result. ....	58

<b>Figure 31:</b> The growth trajectory for different seed distribution width which is used for minimizing weight coefficient of variation result. ....	59
<b>Figure 32:</b> Final crystal size distribution for minimizing weight coefficient of variation. ....	61
<b>Figure 33:</b> The concentration trajectory for different seed distribution width which is used for minimizing weight coefficient of variation result. ....	62
<b>Figure 34:</b> The growth rate for different $j$ . ....	66
<b>Figure 35:</b> The concentration trajectory for different $j$ value. ....	70
<b>Figure 36:</b> Final crystal size distribution for different $j$ value. ....	71
<b>Figure 37:</b> Different moment during the batch for different $j$ value. ....	72



## List Of Tables

**Table 1:** Parameters that for simulated annealing ..... 20

**Table 2:** Objective functions used from literature..... 25



# 1. Introduction

## 1.1. Overview

Crystallization is a widely used solid liquid separation process. It occurs when the solute concentration exceeds the saturation concentration. We define the supersaturation as the difference between the solute concentration and the saturated solute concentration. The supersaturation can be made by cooling the system, evaporating the solvent from system or adding compound that decreases the saturation concentration of the solute. When in process, the supersaturation usually is controlled in metastable region. The metastable region is shown in Figure 1. When the supersaturation is under metastable region, the crystal starts to dissolve. On the other hand, when the supersaturation exceeds the metastable region, a large amount of nucleation would occur.

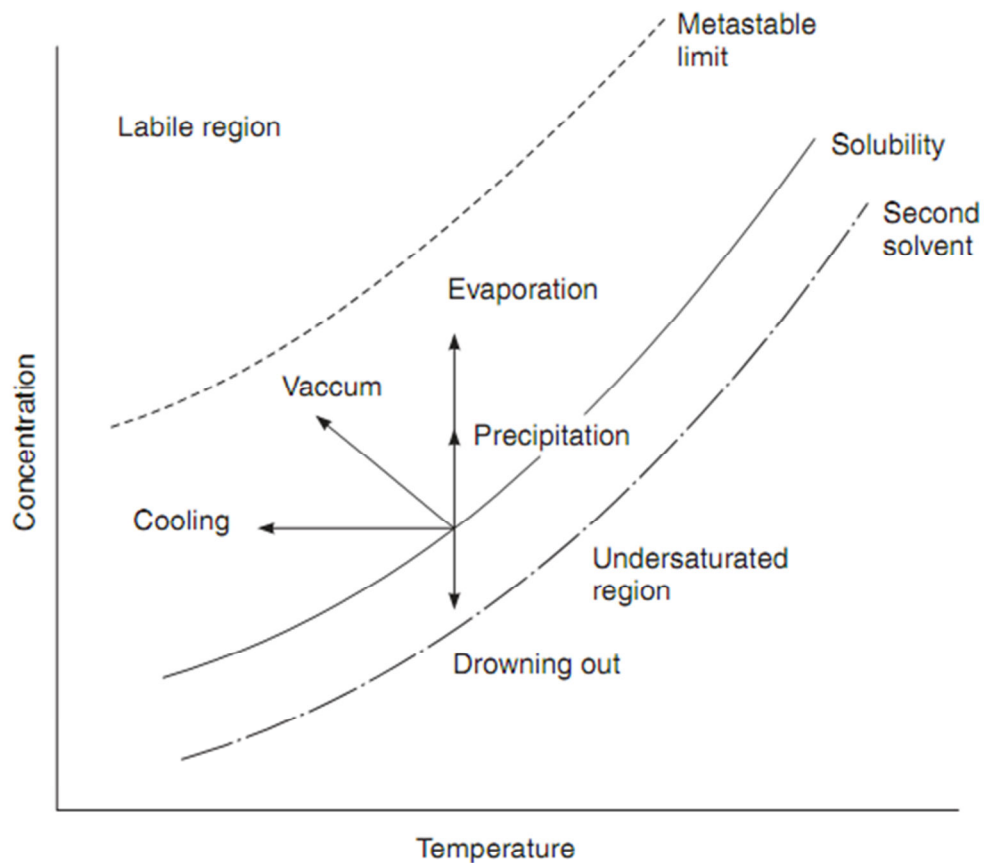


**Figure 1:** Supersaturation and metastable zone. [1]

The driving force of crystallization - supersaturation causes two phenomena: crystal growth and crystal nucleation. The previous one makes crystal become bigger. Another one makes more crystals. There are two kinds of nucleation, one is primary nucleation, and another one is secondary nucleation. The primary nucleation happens whether or not the suspend crystal exists. The secondary nucleation is used to describe the nucleation only when

the suspend crystal exists. In this work, the batch process starts with seed crystal. So the secondary nucleation is the major nucleation mechanism.

Another phenomenon is crystal growth. The crystal growth will increase the size of the crystal, both seeded crystal and nucleated crystal. In reality, if the supersaturation is increasing, both nucleation rate and growth rate would increase. But the magnitude of increase for nucleation rate is larger than growth rate. Therefore, if we want to suppress the nucleation rate when keeping the crystal growth, we can keep the supersaturation value low in entire process. However, if we do so, the entire process would take too much time.

A good process is to produce desired crystal size distribution (CSD), because it is not only the quality of the product, but also influences the efficiency of the downstream process like filtration or drying. However, there are different ways to evaluate how good the product CSD is due to different situation. Researchers use different objective functions to optimize the process for different needs of the process. These objective functions are things to be focus in this work.



## 1.2. Literature Survey

Batch crystallization is a widely used liquid solid separation process. The system can be described by mass balance and population balance. After the work of Jones (1974) [2], many researchers use moment transformation to study this system. Ward et al. developed a dimensionless model based on moment transformation, which helps to develop an imperial concept that is not specific to any solute-solvent system.

There are two ways to optimize a batch crystallizer. One is by optimizing the seeding (Kubota and Doki et al. [3], Lung-Somarriba et al. [4], Hojjati and Rohani [5] and Chung et al. [6]). Another way is optimizing the temperature trajectory. At 1974, Jones et al.[2] compare the result from nature cooling, linear cooling and constant nucleation rate cooling and conclude that controlled cooling significantly reduce the nucleation and enlarger the larger crystal.

Due to the high non-linearity of the crystallization mathematical model, pioneer researcher developed some approximate trajectory instead of optimizing the temperature. Mullin and Nyvlt[7] developed a trajectory based on the assumption of negligible nucleation and constant supersaturation, it has a great advantage that the trajectory can be determined with only the mass of the seed, the initial and final concentration and the batch time. Chung et al. [6]

optimize both the temperature trajectory and the seeding parameters with dynamic programming framework. Ward et al.[9] optimized the growth trajectory (supersaturation profile) by sequentially iteration. However, due to the convex nature of the system, when using different objective functions, the system may not converge. Moreover, with different initial guesses, sometimes the system will converge to a local minimum. Choong et al.[8], applied simulated annealing for the optimization of crystallization systems. This method is widely used for non-linear systems. Simulated annealing is also being known as a method that can often find the global minimum in non-convex problems. It is the optimization strategy used in this work.

Some researchers consider multiple objective function, usually combining them into one objective using a weighted sum. For example, when the goal is to minimize both weight mean size of the crystal and the mass of the nucleated crystal, the objective function may become “minimizing weight mean size plus mass of the nucleated crystal.” In this example the weighting factor for the weight mean size and the mass of the nucleated crystal both is one. If minimizing mass of the nucleated crystal is more important, weighting factor for it would be higher than other. Then the problem is to determine the weighting factor for each objective.

Another approach for consider multiple objectives is to determine the so-called Praeto-optimal front. Sarkar et al.[24] proposed to use genetic algorithm to solve these kind of multi objective function problem. They use genetic algorithm to generate an optimal solution set with a Praeto-front. Once the Praeto-optimal solution is achieved, the user can visualize the trade-off between objectives and choose an operate point. However, when it comes to three objective functions or more, it is hard to visualize the optimal solution from Praeto-optimal solution figure. Furthermore because the genetic algorithm is mapping through different weighting factors of objective functions, it cost more time than solving the problem using a single objective function.

One objective function may correlate closely with another objective function. For example, optimize with objective function “minimizing mass of the nucleated crystals” would achieve a similar result as using the objective function “maximizing weight mean size of the crystals.” That is because the general goal of these two objective functions is suppressing nucleation. In reality, nucleated crystals are undesirable. Most objective functions considered in the literature are concerned with suppressing the nucleation. In this work, we are collect the objective function that have been used by and compare them by comparing the results of using each objective function. The goal is to see

whether there is one single objective function that works well for many purposes.



## 2. Dimensionless Model

### 2.1. Dimensionless Moment Equations

Without agglomeration and breakage, for a well-mixed batch crystallizer, the population balance can be expressed like this:

$$\frac{\partial f(L,t)}{\partial t} + \frac{\partial (G(L,t) f(L,t))}{\partial L} = 0 \quad (1)$$

Where  $f(L,t)$  is the crystal size distribution (CSD) function,  $B$  (#/m<sup>3</sup>s) and  $G$  (m/s) are nucleation rate and growth rate, respectively. A left boundary condition could be applied:

$$f(0,t) = \frac{B(f(L,t),t)}{G(0,t)} \quad (2)$$

Here is the definition of moments of CSD:

$$\mu_i = \int_0^{\infty} L^i f(L) dL \quad i = 0, 1, 2, \dots \quad (3)$$

A population balance equation with moments can be shown like this:

$$\frac{d\mu_0}{dt} = B \quad (4)$$

$$\frac{d\mu_i}{dt} = iG\mu_{i-1} \quad i = 1, 2, \dots \quad (5)$$

The nucleated crystals (subscript n) and the seed-grown crystals (subscript s) are tracked individually. The population moment equation for the seed-grown crystal can be described like this:

$$\frac{d\mu_{s,0}}{dt} = 0 \quad (6)$$

$$\frac{d\mu_{s,i}}{dt} = iG\mu_{s,i-1} \quad i = 1, 2, \dots \quad (7)$$

And for the nucleated crystal:

$$\frac{d\mu_{n,0}}{dt} = B \quad (8)$$

$$\frac{d\mu_{n,i}}{dt} = iG\mu_{n,i-1} \quad i = 1, 2, \dots \quad (9)$$

The crystallization process is driven by supersaturation. It is the difference of current concentration and saturated concentration.

$$S = C - C_{\text{sat}} \quad (10)$$

The concentration can be measured by mass balance.

$$\frac{dC}{dt} = -3G\rho_c k_v \mu_3 \quad (11)$$

Where  $\rho_c$  is the crystal density and  $k_v$  is the crystal volumetric shape factor. A common expression for crystal growth rate and secondary nucleation rate are:

$$G = k_g S^g \quad (12)$$

$$B = k_b G^\gamma \mu_3 \quad (13)$$

where  $k_g$ ,  $g$ ,  $k_b$  and  $\gamma$  are kinetic parameters. To generalize the analysis, the equations from 4 to 11 are non-dimensionalized.

We define:

$$C' = \frac{C - C_f}{C_0 - C_f} \quad (14)$$

$$t' = t/t_f \quad (15)$$

Where  $t_f$  is the total batch time, and  $C'$  is the dimensionless concentration which decreases from 1 to 0 during the batch. We also define the dimensionless  $G$  and  $B$

$$G' = \frac{G}{\bar{G}} \quad (16)$$

$$\bar{G} = (k_b t_f^4)^{\frac{-1}{\gamma+3}} \quad (17)$$

$$B' = \frac{B}{\bar{B}} = \frac{B}{k_b \bar{\mu}_3 (k_b t_f^4)^{\frac{-\gamma}{\gamma+3}}} \quad (18)$$

$$\bar{B} = k_b \bar{\mu}_3 (k_b t_f^4)^{\frac{-\gamma}{\gamma+3}} \quad (19)$$

From the concept of mass balance, we define:

$$\mu'_3 = \frac{\mu_3}{\bar{\mu}_3} \quad (20)$$

$$\bar{\mu}_3 = \frac{C_0^\dagger}{\rho_c k_v} = \frac{(C_0 - C_f)}{\rho_c k_v} \quad (21)$$

To simplify Equation 5, we also define:

$$\bar{\mu}_0 = \bar{B} t_f \quad (22)$$

$$\bar{\mu}_1 = \bar{B} \bar{G} t_f^2 \quad (23)$$

$$\bar{\mu}_2 = \bar{B} \bar{G}^2 t_f^3 \quad (24)$$

$$\bar{\mu}_3 = \bar{B} \bar{G}^3 t_f^4 \quad (25)$$

The differential equations becomes:

$$\frac{d\mu'_0}{dt'} = B' = (G')^z (\mu'_3) \quad (26)$$

$$\frac{d\mu'_1}{dt'} = G' \mu'_0 \quad (27)$$

$$\frac{d\mu'_2}{dt'} = 2G' \mu'_1 \quad (28)$$

$$\frac{d\mu'_3}{dt'} = 3G' \mu'_2 \quad (29)$$





## 2.2. Seed

It is desirable to use monodisperse seed, which means all of the seed crystal are in the same size. In fact, it is hard to prepare a perfectly monodisperse seed crystals. We consider a polyidisperse seed CSD base on a parabolic function.

$$f_0(L) = \begin{cases} 0 & L < x_0 - w/2 \\ -a \left( L - \left( x_0 - \frac{w}{2} \right) \right) \left( L - \left( x_0 + \frac{w}{2} \right) \right) & x_0 - w/2 \leq L \leq x_0 + w/2 \\ 0 & L > x_0 + w/2 \end{cases} \quad (30)$$

Where  $x_0$  and  $w$  are mean size and width of seed CSD, as shown in

Figure 2.

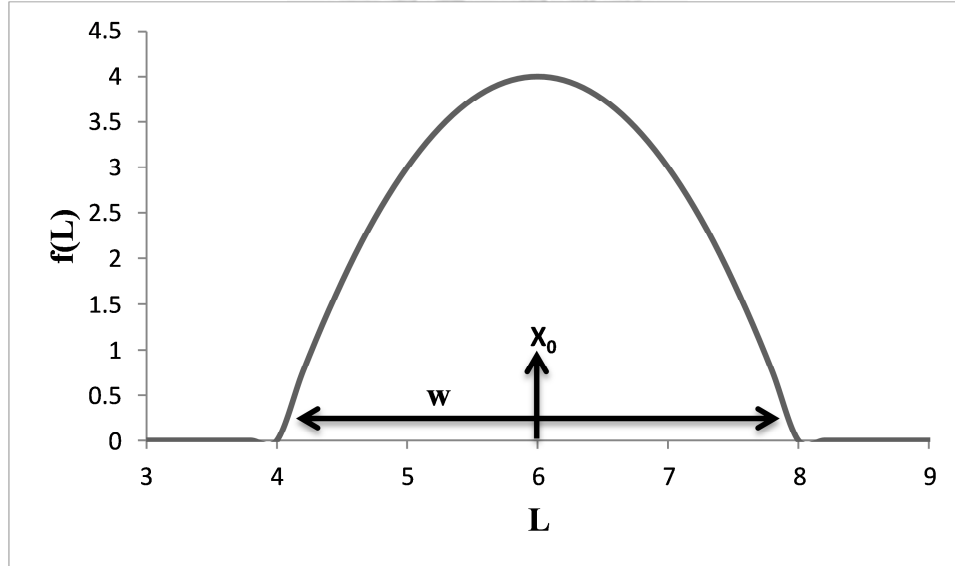


**Figure 2:** The parabolic seed crystal size distribution (CSD) function.

In order to reach the total mass of the seeds  $m_s$ , the variable  $a$  must satisfy

this condition:

$$\int_0^{\infty} L^3 f_0(L) = \int_{x_0-w/2}^{x_0+w/2} L^3 f_0(L) = \frac{m_s}{\rho k_v} \quad (31)$$

Where  $m_s$  is the mass of seeds,  $\rho$  is density of crystal,  $k_v$  is shape

factor. Solving the equation we get:

$$a = \frac{m_s}{\rho_c k_v} \left( \frac{1}{6} x_0^3 w^3 + \frac{1}{40} x_0 w^5 \right)^{-1} \quad (32)$$

Therefore:

$$f_0(L) = -\frac{m_s}{\rho_c k_v} \left( \frac{1}{6} x_0^3 w^3 + \frac{1}{40} x_0 w^5 \right)^{-1} \left( L - \left( x_0 - \frac{w}{2} \right) \right) \left( L - \left( x_0 + \frac{w}{2} \right) \right) \quad (33)$$

for  $x_0 - w/2 \leq L \leq x_0 + w/2$ .

Define:

$$m'_s = \frac{m_s}{C_0 - C_f} \quad (34)$$

$$x'_0 = \frac{x_0}{G t_f} \quad (35)$$

$$L' = \frac{L}{G t_f} \quad (36)$$

$$w' = \frac{w}{\bar{G}t_f} \quad (37)$$

$$f'(L, t) = \frac{\bar{G}f(L, t)}{\bar{B}} \quad (38)$$

Substituting the definitions of dimensionless relationship into Equation 33, we will get:

$$f'_0(L') = -m'_s \left( \frac{1}{6} x_0'^3 w'^3 + \frac{1}{40} x_0' w'^5 \right)^{-1} \left( L' - \left( x_0' - \frac{w'}{2} \right) \right) \left( L' - \left( x_0' + \frac{w'}{2} \right) \right) \quad (39)$$

From the definition of the moments from Equation 3, the dimensionless moments of seed CSD are given by:

$$\mu'_{s,0}(0) = \frac{20m'_s}{x_0'(20x_0'^2 + 3w'^2)} \quad (40)$$

$$\mu'_{s,1}(0) = \frac{20m'_s}{(20x_0'^2 + 3w'^2)} \quad (41)$$

$$\mu'_{s,2}(0) = \frac{m'_s(20x_0'^2 + w'^2)x'_0}{(20x_0'^2 + 3w'^2)} \quad (42)$$

$$\mu'_{s,3}(0) = m'_s \quad (43)$$

At the end of the batch, the total third moment (including the seed crystals and nuclei) of the CSD is:

$$\mu_3(t_f) = \frac{m_s + (C_0 - C_f)}{\rho_c k_v} \quad (44)$$

$$\mu'_3(t_f) = \frac{\mu_3(t_f)}{\bar{\mu}_3} = \frac{m_s + (C_0 - C_f)}{(C_0 - C_f)} = m'_s + 1 \quad (45)$$

### 3. Optimization by Simulated Annealing

Stimulated annealing is a widely used optimization strategy for non-linear systems. It has the advantage that is the re-annealing mechanism, which helps to find the global minimum. In this work, all of the optimization is done using the stimulated annealing toolbox in MATLAB.

#### 1.1. Simulated Annealing

Simulated annealing is a method that emulates the annealing of metal. When annealing a metal, the metal is heated and melted. The high temperature gives energy to the metal atoms so that they can move in the metal. After the heating, the metal is cooled. If the cooling rate is fast, defects may form. In nature a defect means a higher energy state. If the cooling rate is slow, then there is more chance for the atoms to arrange more into a lower-energy structured crystal. A well-formed lattice structure means that the metal is in lower energy state. The entire heating and cooling process make the metal change the arrangement from higher energy state to lower energy state.

To develop an analog to the physical annealing, a variable  $T_a$  is defined that mimics the physical temperature. The annealing temperature affects two aspects of the simulation. One is the changing of the point. At higher annealing

temperature, the distance between current and next tried point will be larger. Another one is the likelihood of accepting a higher energy state. At higher temperature, the system will be more likely to accept a state with higher objective value.

Simulated annealing is widely used because of its ability to avoid local minima. As shown in Figure 3, the vertical axis is the objective function value. There is a local minimum here shown as point A, and there also is a global minimum shown as point B. The current state is point C. In a traditional minimum finding algorithm, there is no mechanism to accept a worse result. That means that from the current state point C, the algorithm can only move downward. It will find a minimum value, but the minimum is a local minimum. The initial guess becomes very important. If the initial guess is near the global minimum, then the result may be the global minimum. Otherwise, the algorithm would find a local minimum. By contrast, the simulated annealing algorithm has a mechanism to accept a worse result. As shown in Figure 3, both simulated annealing algorithm and other algorithm will accept point D, because it has lower objective function value. However, point E has an undesirable higher objective function value. In the simulation annealing algorithm there is a

possibility to accept point E, and it depends on the current annealing temperature. Once the state reaches the hill at point E, the algorithm then has a chance to reach point F and then the global minimum point B.

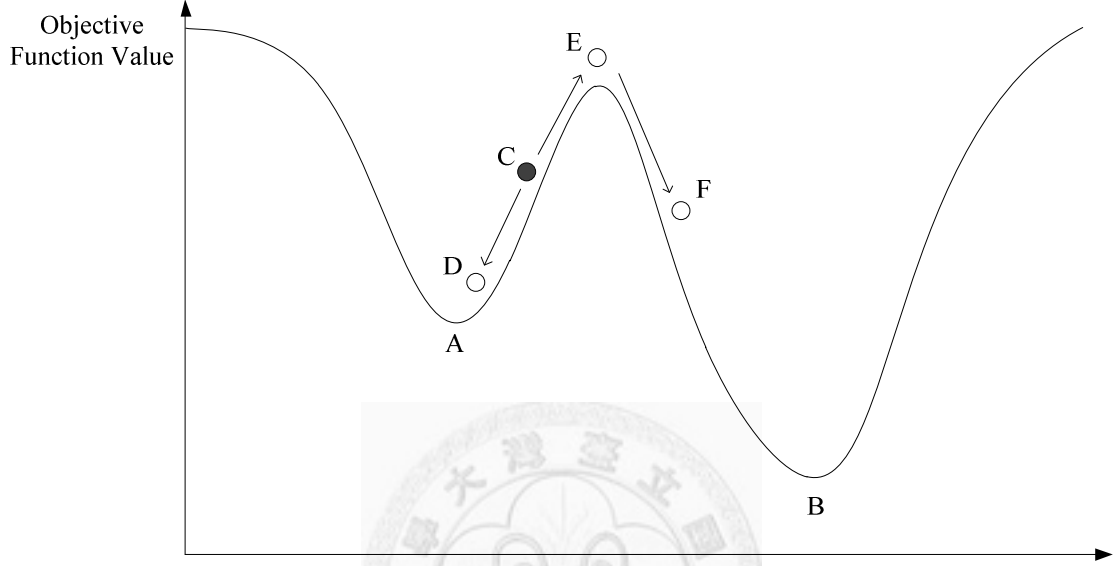


**Figure 3:** Representation of optimization by simulated annealing.

The algorithm is shown in Figure 5. Initially the growth trajectory is a random function provided by MATLAB. The initial annealing temperature we use is 10. The next step is to determine the annealing temperature at the iteration time. The annealing temperature is a function of iteration time ( $k_{sa}$ ). In this work, the annealing temperature function can be express by:

$$T_a(k_{sa}) = T_{ini} \times 0.99^{\text{mod}(k_{sa}, k_r)} \quad (46)$$

Where “mod “ is the modulus function, and  $k_r$  is the number of iterations until the temperature goes back to initial temperature ( $T_{ini}$ ). A plot of the annealing temperature versus time is shown in Figure 4 for  $k_r = 2500$ .

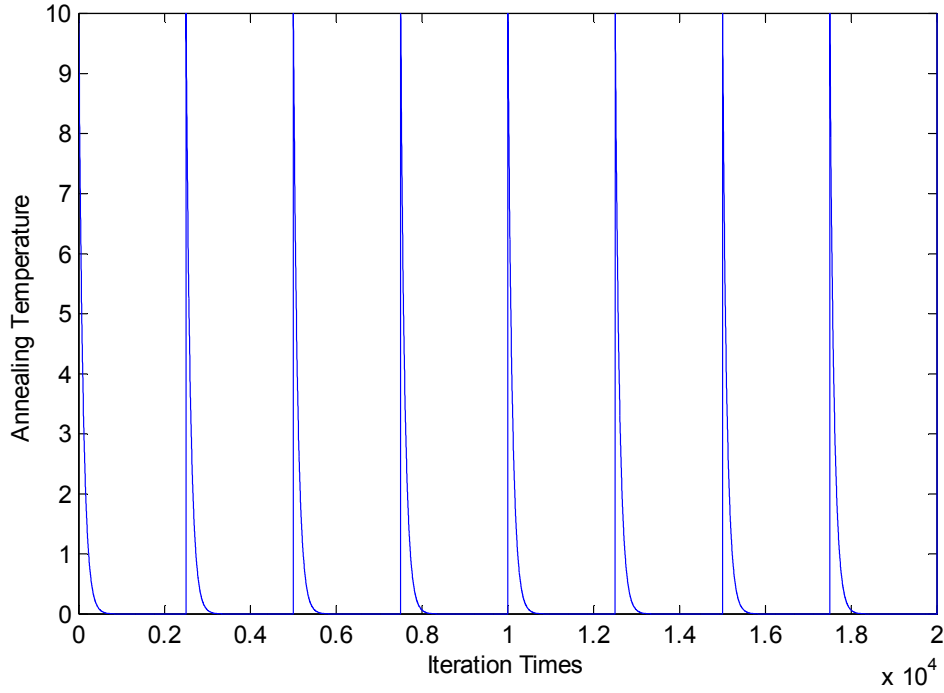


**Figure 4:** The annealing temperature.

The reason of choosing this kind of annealing temperature is that although the code from MATLAB has a re-annealing mechanism to make the algorithm jump out of the local minimum, it is still not enough. So we don't use the default annealing function but instead construct an annealing temperature profile that reheats the system after  $k_r$  iterations.

After the new annealing temperature is determined, as shown in Figure 5, we propose a new growth trajectory according to the annealing temperature. The higher the annealing temperature, the larger the changing between new trajectory and previous trajectory. The next step is to normalize the growth trajectory such that at the end of the batch, the value of the third moment ( $\mu'_3$ ) equal to  $m'_s + 1$ , according to the mass constraint.

With the new growth trajectory we can run the batch to determine the final crystal moments and the objective function value. The next step is to compare the objective function value from new growth trajectory and previous growth trajectory. There will be two situations: the new objective value may be higher or lower than the previous one. Our goal is to minimize the objective function, so if the objective value from new growth trajectory is lower than the previous one, we accept it with no doubt. On the other hand, if the new objective value is higher than the previous one, it still may be accepted. In the code provided in the MATLAB toolbox, the possibility of acceptance equation is like this:

$$P(t) = \frac{1}{1 + \exp\left(\frac{\Delta}{T_a}\right)} \quad (47)$$



Where  $\Delta$  is the difference between previous and new objective function value. It is a positive value.  $T_a$  is the annealing temperature. The possibility of acceptance is between 0 and 0.5. Larger  $\Delta$  value will cause smaller acceptance possibility. If the new growth trajectory is rejected, the program will keep the previous growth trajectory for the next run.

The stop criterion is defined by the iteration time. We set the maximum number of iteration to 30000, the program will give the result and end after the iteration times is over 30000. Table 1 shows the parameters we used for the code provided from MATLAB in this work. For parameter that are not listed in this table, the default setting is used.

**Table 1:** Parameters that for simulated annealing

Parameter	Value
Lower bound	0
Upper bound	100
Initial temperature	10
Temperature function	Equation 46
Reannealing interval	300
Maxiter	30000

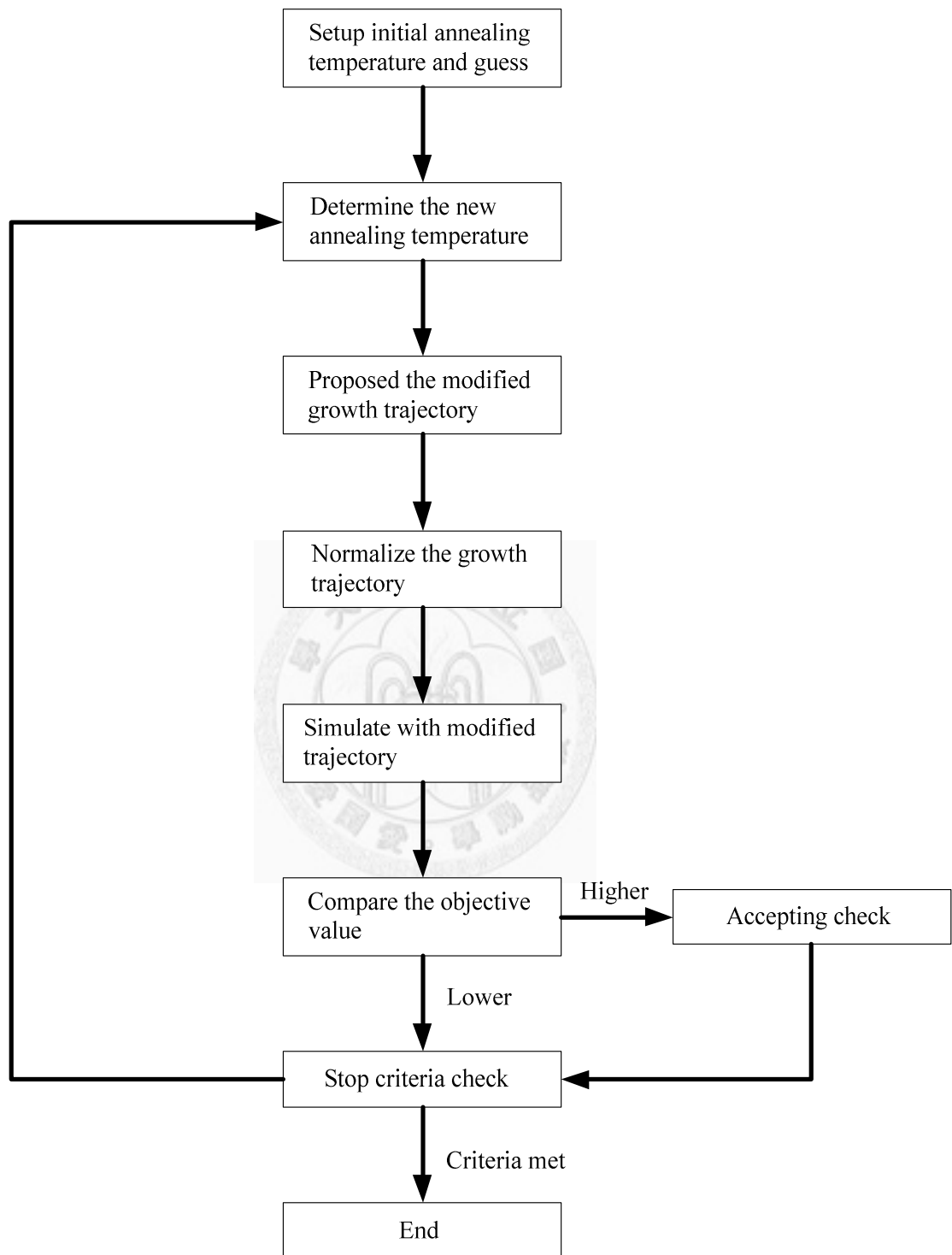


**Figure 5:** Simulation annealing algorithm.

#### 4.1. Control Variable

In this work the control variable is the growth trajectory ( $G'(t')$ ). There are two reasons that we do not use the temperature trajectory as the control variable. One is that using temperature trajectory as control variable makes finding a solution more difficult. Another reason is that solubility parameters are required to determine the relationship between temperature trajectory and growth trajectory. If we need the solubility parameters, the result is no longer general to many different systems.

After the optimal growth trajectory is found, the optimal supersaturation trajectory can be determined using Equation 12. We can also find the concentration trajectory by mass balance. Combining the supersaturation and the concentration trajectory we can achieve the saturated concentration trajectory. Applying the solubility parameters to the saturated concentration trajectory, we can have the temperature trajectory.

#### 4.2. Final Mass Constraint

In this work the initial concentration and the final concentration are fixed.

To ensure the final concentration to be the same after every simulation, a

constraint is added. From mass balance, the solution concentration directly related to the mass of the crystal in the batch crystallizer. And for the dimensionless model, this constraint make the value of the third moment ( $\mu'_3$ ) to be  $m'_s + 1$  at the end of the batch, as shown in Equation 44 and Equation 45.

During the simulation, we define the growth trajectory like this:

$$G(t) = G_0 \times aa \quad (48)$$

where  $G(t)$  is growth rate trajectory, and  $aa$  is the normalized growth trajectory, which is a  $1 \times 25$  spline matrix with underneath area equal to one. It is also the input variable for simulated annealing program. And  $G_0$  is a multiplying factor adjusted to meet the final mass constraint. To ensure the final mass constraint is met,  $G_0$  is recalculated every time after the growth trajectory is changed.

## 4. Discussion

### 4.1. Objective Function Classification

From Table 2, commonly-used objective functions can be classified into three types: crystal mean size type, single moment type and coefficient of variation type. Within the crystal mean size type, commonly-used objective functions are maximizing the number mean size ( $\mu_{T1}/\mu_{T0}$ ) and the weight mean size ( $\mu_{T4}/\mu_{T3}$ ). Within the single moment type are objectives that minimize a single moment of the nucleated crystals ( $\mu_{n3}, \mu_{n2}, \mu_{n1}, \mu_{n0}$ ). Within the coefficient of variation type are objectives of minimizing the number based coefficient of variation ( $\sqrt{\mu_{T2}\mu_{T0}/\mu_{T1}^2 - 1}$ ) and weight based coefficient of variation ( $\sqrt{\mu_{T5}\mu_{T3}/\mu_{T4}^2 - 1}$ ).

**Table 2:** Objective functions used from literature.

Objective to minimize	Reference
$\mu_{n3}$	9
$\mu_{n3}$	10
$\mu_{n3}$	11
$\frac{\mu_2}{\mu_0} - \left( \frac{\mu_1}{\mu_0} \right)^2 - \alpha \left( \frac{\mu_1}{\mu_0} \right)$	12
$\frac{\mu_{n3}}{\mu_{s3}}$	13
$-\frac{\mu_4}{\mu_3}$	6
$\left( \frac{\mu_2 \mu_0}{\mu_1^2} - 1 \right)^2$	6
$-\mu_{s1}$	14
$-\frac{\mu_1}{\mu_0}$	15
$\left( \frac{\mu_5 \mu_3}{\mu_4^2} - 1 \right)^2$	16
$(f\text{-lognormal\_f})^2 + \text{vairance}$	17
$\frac{B}{G}, \frac{\mu_{n3}}{\mu_{s3}}, \sqrt{\frac{\mu_5 \mu_3}{\mu_4^2} - 1}$	18
$\frac{B}{G}, \frac{\mu_{n3}}{\mu_{s3}}, \sqrt{\frac{\mu_5 \mu_3}{\mu_4^2} - 1}$	19
$\mu_{n3} - \mu_{s3}, \mu_{n3}$	20
$-\frac{\mu_1}{\mu_0}$	21

**Table 2(continued):** Objective functions used from literature.

Objective to minimize	Reference
$-\frac{\mu_4}{\mu_3}$	22
(gained mass-seed mass)/time	23
$-\frac{\mu_4}{\mu_3}, \mu_{n3}, \text{batch\_time}, \sqrt{\frac{\mu_5\mu_3}{\mu_4^2} - 1}$	24
Standard deviation, $\sqrt{\frac{\mu_2\mu_0}{\mu_1^2} - 1}$	25
$\sum [CSD - \text{DesireCSD}]^2$	26
$-\frac{\mu_4}{\mu_3}$	27
$-\frac{\mu_4}{\mu_3}, \sqrt{\frac{\mu_5\mu_3}{\mu_4^2} - 1},$	28
$-\frac{\mu_4}{\mu_3} - \frac{\alpha}{t_f}$	
$-\frac{\mu_4}{\mu_3}, \sqrt{\frac{\mu_5\mu_3}{\mu_4^2} - 1}$	29
$-\frac{\mu_4}{\mu_3}, \frac{\mu_{n3}}{\mu_{s3}}$	30
$-\frac{\mu_4}{\mu_3}, \sqrt{\frac{\mu_2\mu_0}{\mu_1^2} - 1}, \frac{\mu_{n3}}{\mu_{s3}}$	31
$-\frac{\mu_4}{\mu_3}, \sqrt{\frac{\mu_2\mu_0}{\mu_1^2} - 1}, \frac{\mu_{n3}}{\mu_{s3}}$	32



## 4.2. Comparison Method

In order to compare these objective functions and try to determine which is most suitable, we determine the optimal saturation trajectory using each objective function and compare the results. In every case, we are able to identify a saturation concentration trajectory that minimizes each objective function. However, some of the objective functions give rise to saturation concentration trajectories that lead to undesired behavior, such as excessive nucleation. For example, as discussed later, the objective function “minimizing the crystal number coefficient of variation” is minimized by deliberately causing a great deal of nucleation at the beginning of the batch, so that the nuclei grow with a narrow distribution. However, this is presumably not really the desired behavior. In fact, for seeded batch crystallization, it is generally understood that the goal is to grow the seeds while minimizing nucleation. In industrial practice, the product crystals would probably be filtered after crystallization and the fines (nucleated crystals) removed.



Therefore, for each objective function, after the optimal trajectory is determined, we also determine the value of the objective function after the nucleated crystals are removed. If most of the benefit from using a particular objective function is eliminated when the nucleated crystals are removed, then that objective function is considered to be inferior.



### 4.3. Weight COV and Number COV

In Figure 6, upper panel shows the number based crystal size distribution function for result using minimizing weight coefficient of variation and minimizing number coefficient of variation as objective function. In this panel we can see that the distribution of result using minimizing number coefficient of variation is more narrow than distribution of result using objective function minimizing weight coefficient of variation.

Lower panel in Figure 6 shows the weighted final crystal size distribution function, both results from using minimizing weight coefficient of variation and number coefficient of variation shows a peak. And the distribution peak of result using weight coefficient of variation is narrower.

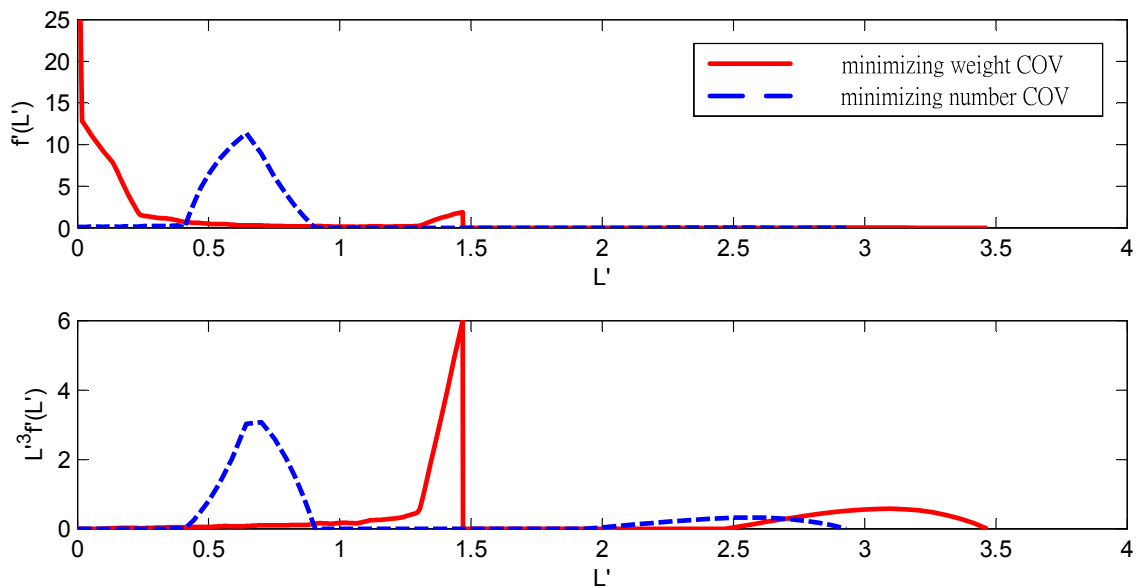


**Figure 6:** Final crystal size distribution for different objectives.

Both results from two objective functions show a narrow peak, however it is the nucleated crystals that give a narrow distribution. Figure 7 shows the optimal growth rate using objective function minimizing weight coefficient of variation and number coefficient of variation. When the supersaturation increases, both nucleation rate and growth rate will be enhanced. From Equation 13, we can see that the growth rate directly affect the nucleation rate. Because of the power in Equation 13  $\gamma$  is equal to three, when the growth rate increases heavily, the nucleation rate increases much more.

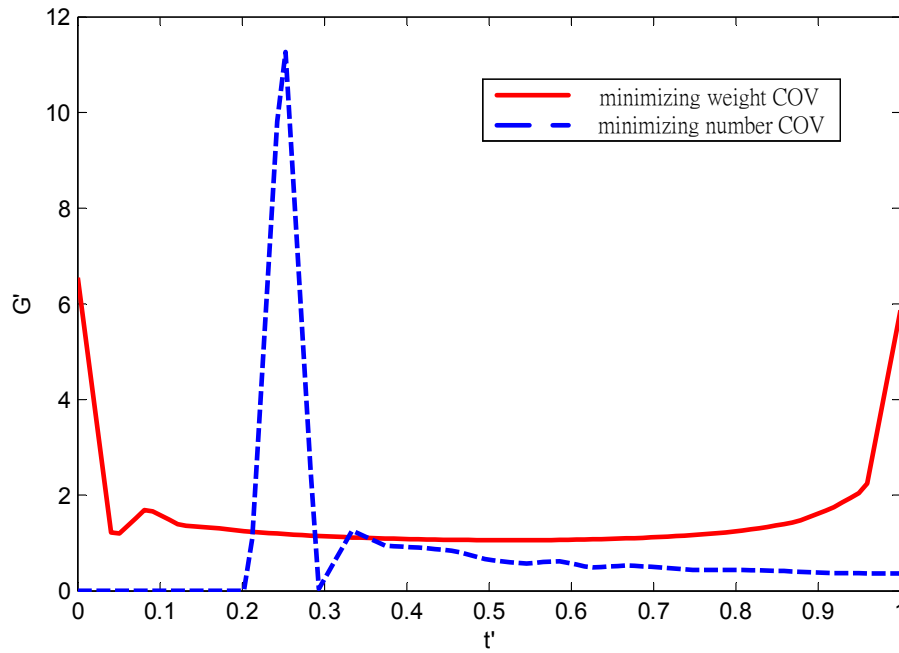


**Figure 7:** The optimal growth trajectory using objective function, minimizing weight coefficient of variation and minimizing number coefficient of variation.

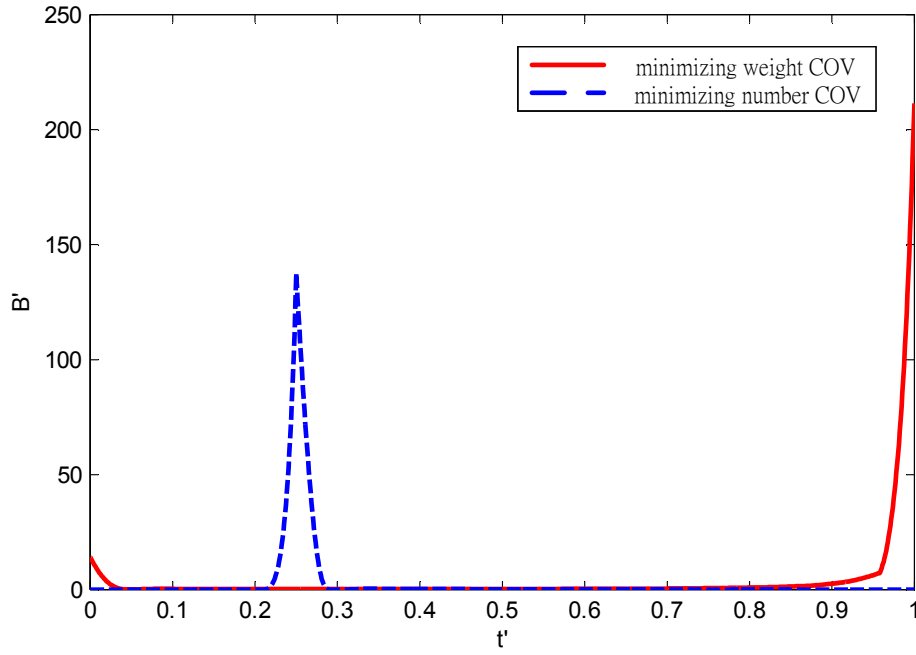


**Figure 8:** The optimal nucleation rate trajectory using objective function, minimizing weight coefficient of variation and minimizing number coefficient of variation.

Figure 8 shows the nucleation rate trajectory. In this figure we can see that both of the objective functions result in large nucleation peak in the process. The objective function minimizing weight coefficient of variation causes excess nucleation at the beginning of the batch, and the objective function minimizing number coefficient of variation causes excess nucleation at the middle of the batch time. From Figures 6, 7 and 8 we can see that these two objective functions achieve narrow final crystal size distribution by making excess nucleation during the batch. Thus they achieve the minimum of

the objective function, however, the large amount of nucleated crystals and excess nucleation are not desirable.

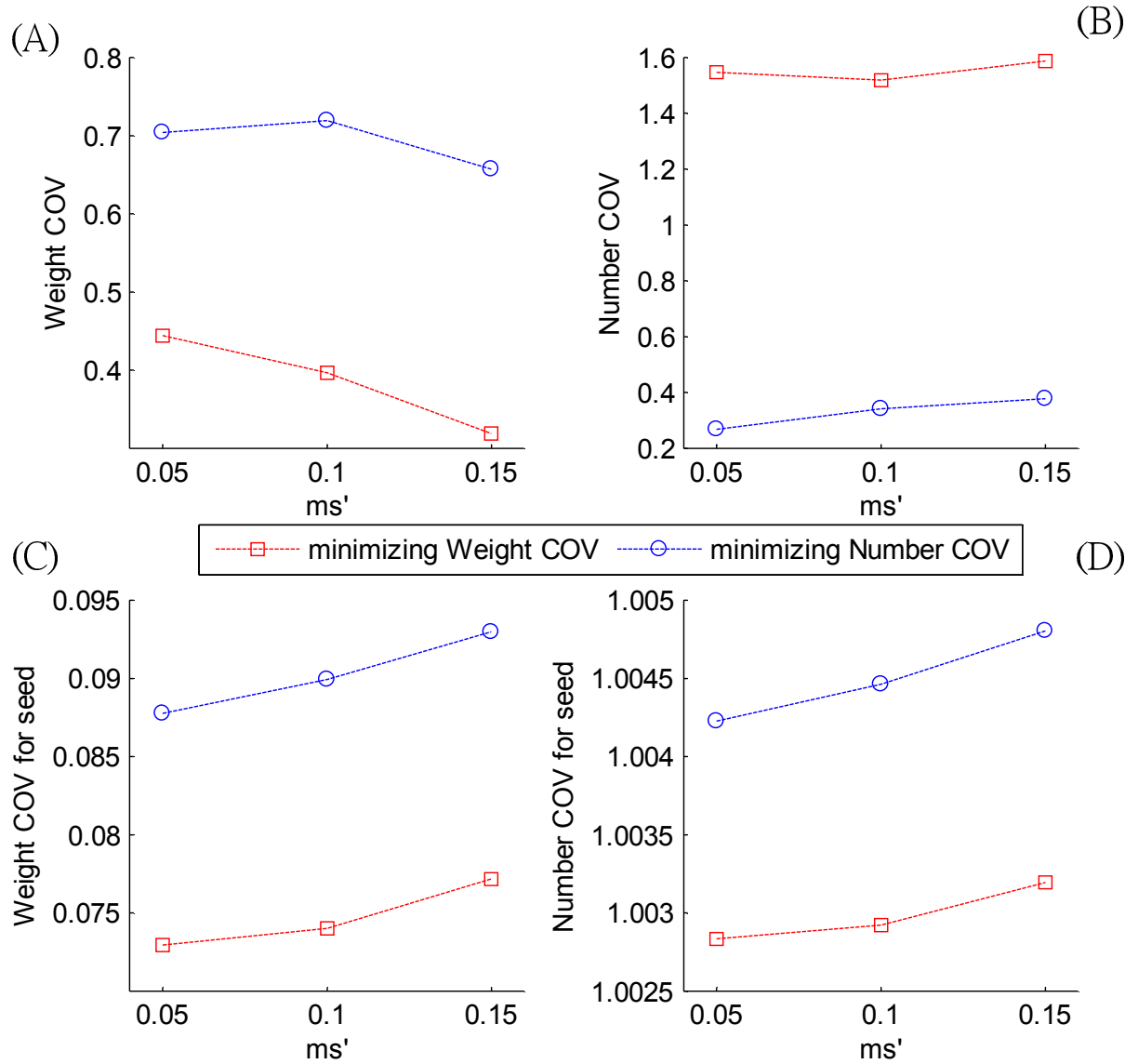


**Figure 9:** Weight coefficient of variation and number coefficient of variation value for different objectives.

Figure 9 shows the resulting weight coefficient of variation and number coefficient of variation when both of these objectives are used as the objective

function. As expected, in panel A, when the objective is to minimize the weight coefficient of variation, the weight coefficient of variation is indeed lower than the number coefficient of variation. In Panel B, again as expected, when the objective is to minimize the number COV, the number COV is indeed less than when the objective is to minimize the weight COV.

However, the situation if the nucleated crystals are filtered out (Panels C and D). In that case, minimizing the weight COV also minimizes the number COV, and using the number COV as the objective results in an inferior performance. Figure 7 shows the number distribution ( $f(l)$ ) and the weight distribution ( $L^3f(L)$ ) of the product using the saturation concentration trajectory that minimizes the weight COV and the number COV. Minimizing the weight COV results in more growth of the seeds. On the basis of these two results, we conclude that among objectives that aim to minimize a COV, minimizing the weight COV is more suitable than minimizing the number COV.

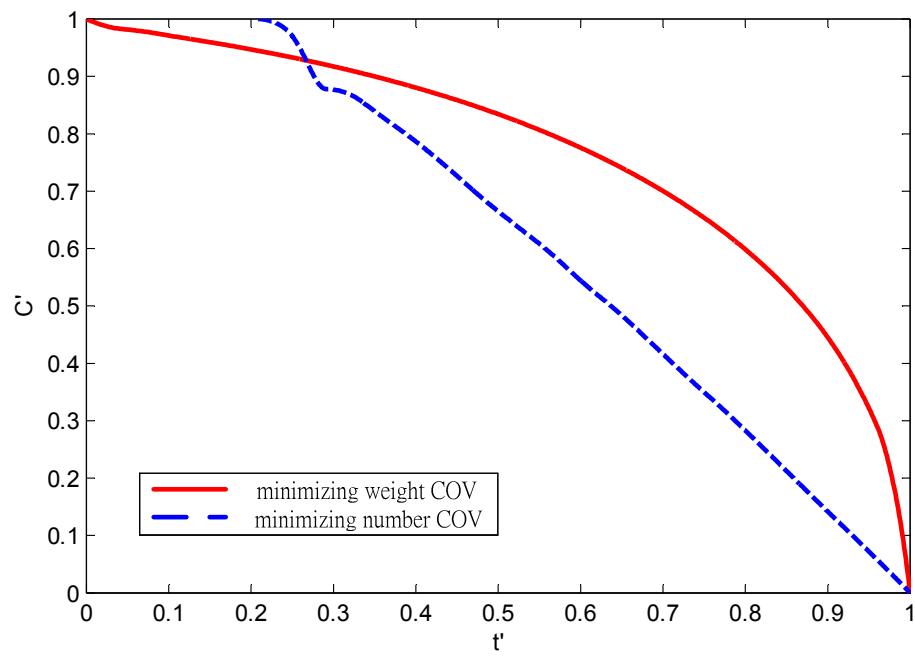


**Figure 10:** The optimal concentration trajectory using objective function, minimizing weight coefficient of variation and minimizing number coefficient of variation.

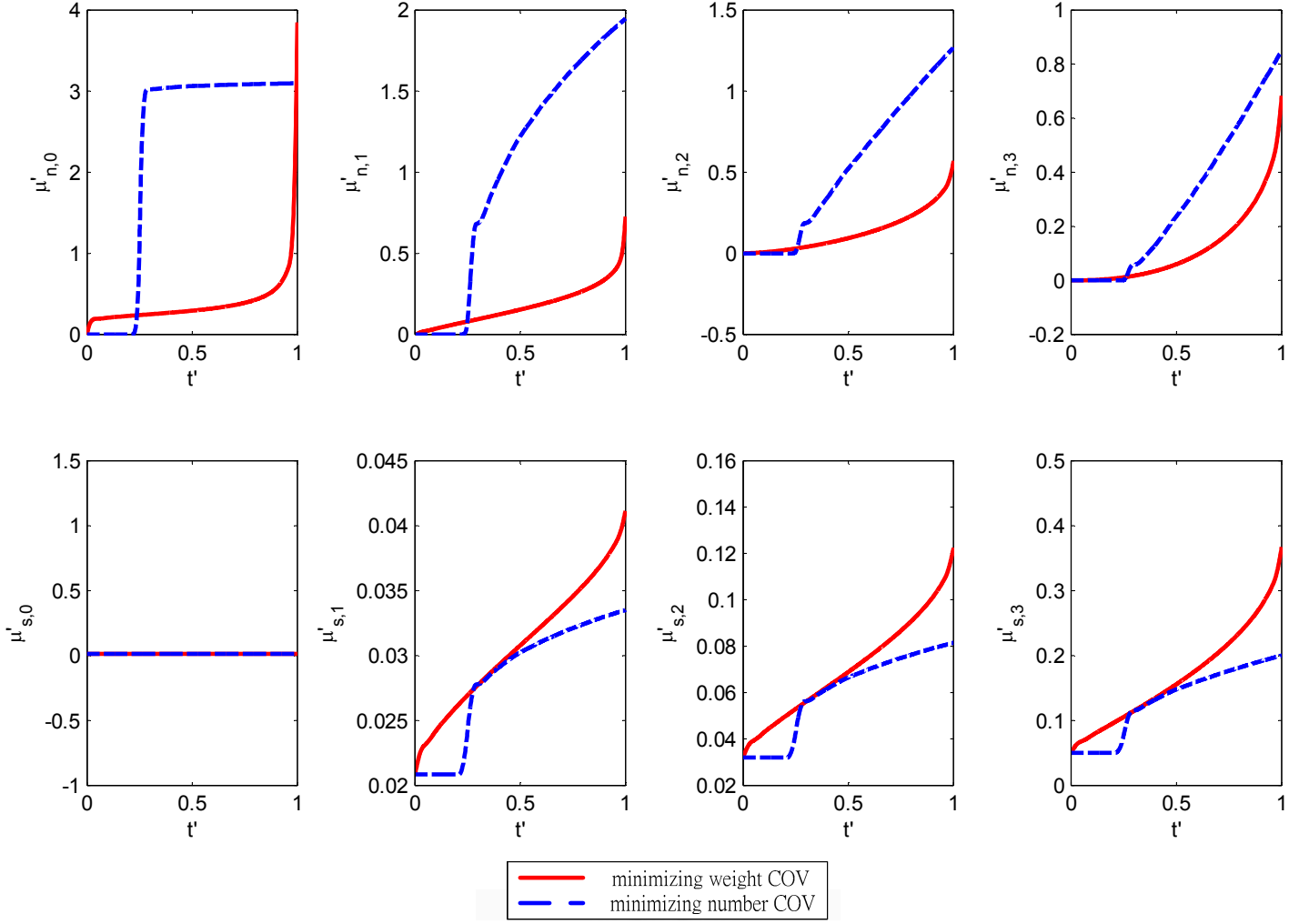


**Figure 11:** Different order of moment plot during the batch time for using objective function minimizing weight coefficient of variation and minimizing number coefficient of variation.



#### 4.4. Weight Mean Size and Number Mean Size

Figure 12 shows the optimal nucleation trajectory using object function minimizing weight mean size and minimizing number mean size. Again we can observer that for trajectory from result using objective function maximizing number mean size causes excess nucleation.

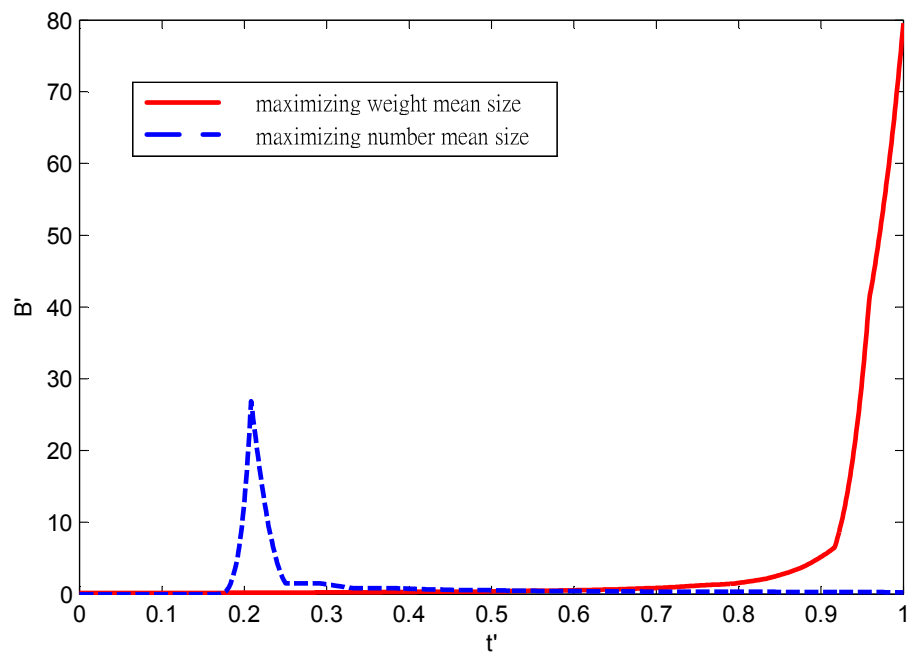


**Figure 12:** The optimal nucleation rate trajectory using objective function, minimizing weight mean size and minimizing number mean size.

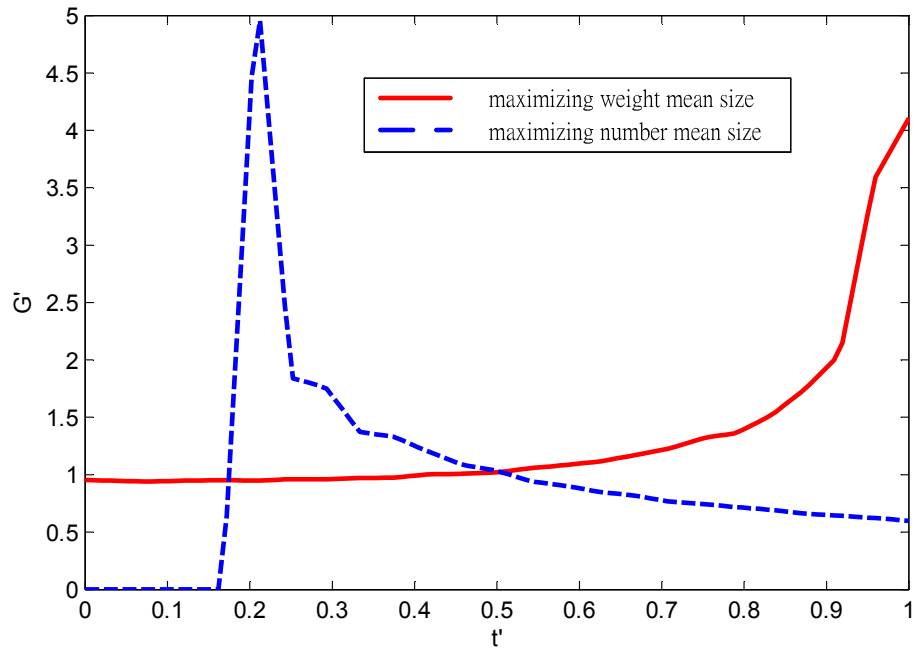


**Figure 13:** The optimal growth trajectory using objective function, minimizing weight mean size and minimizing number mean size.

Figure 13 shows the optimal growth rate trajectory using objective function minimizing weight mean size and minimizing number mean size. We can observe that the batch is actually started when  $t' = 0.16$ .

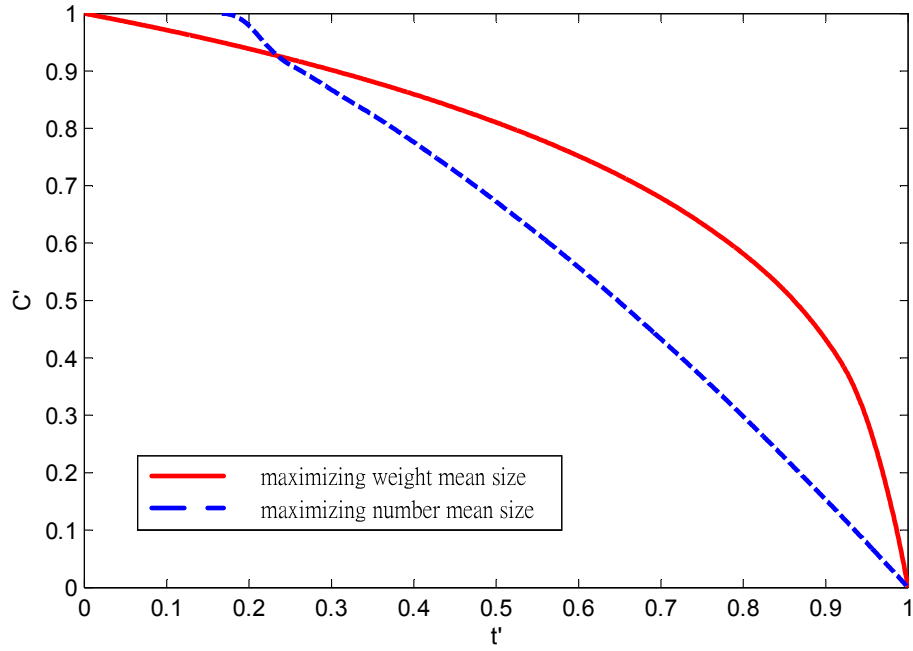


**Figure 14:** The optimal concentration trajectory using objective function, minimizing weight mean size and minimizing number mean size.

Although the optimal trajectory of minimizing number mean size gives an excess early growth and shorten the batch time, it is still reasonable for objective function minimizing number mean size. In Figure 15 we can see that the excess nucleation from trajectory which is optimized using maximizing number mean size causes raising of zeroth moment at the early batch time. However, at the end of the batch the zeroth moment from the optimal trajectory using maximizing weight means size is larger. Since the number mean size of the crystal is defined as  $\mu_{T,1} / \mu_{T,0}$ , the value of the zeroth moment is very important for number mean size when compare to the weight

mean size. And from Equation 26, the nucleation rate directly affects the value of the zeroth moment. Therefore, it is reasonable that the trajectory using maximizing number mean size as objective function by avoiding high growth rate when the third moment is larger at the end of the batch. And that is the major reason why the program chooses an early growth trajectory and shortens the batch time.



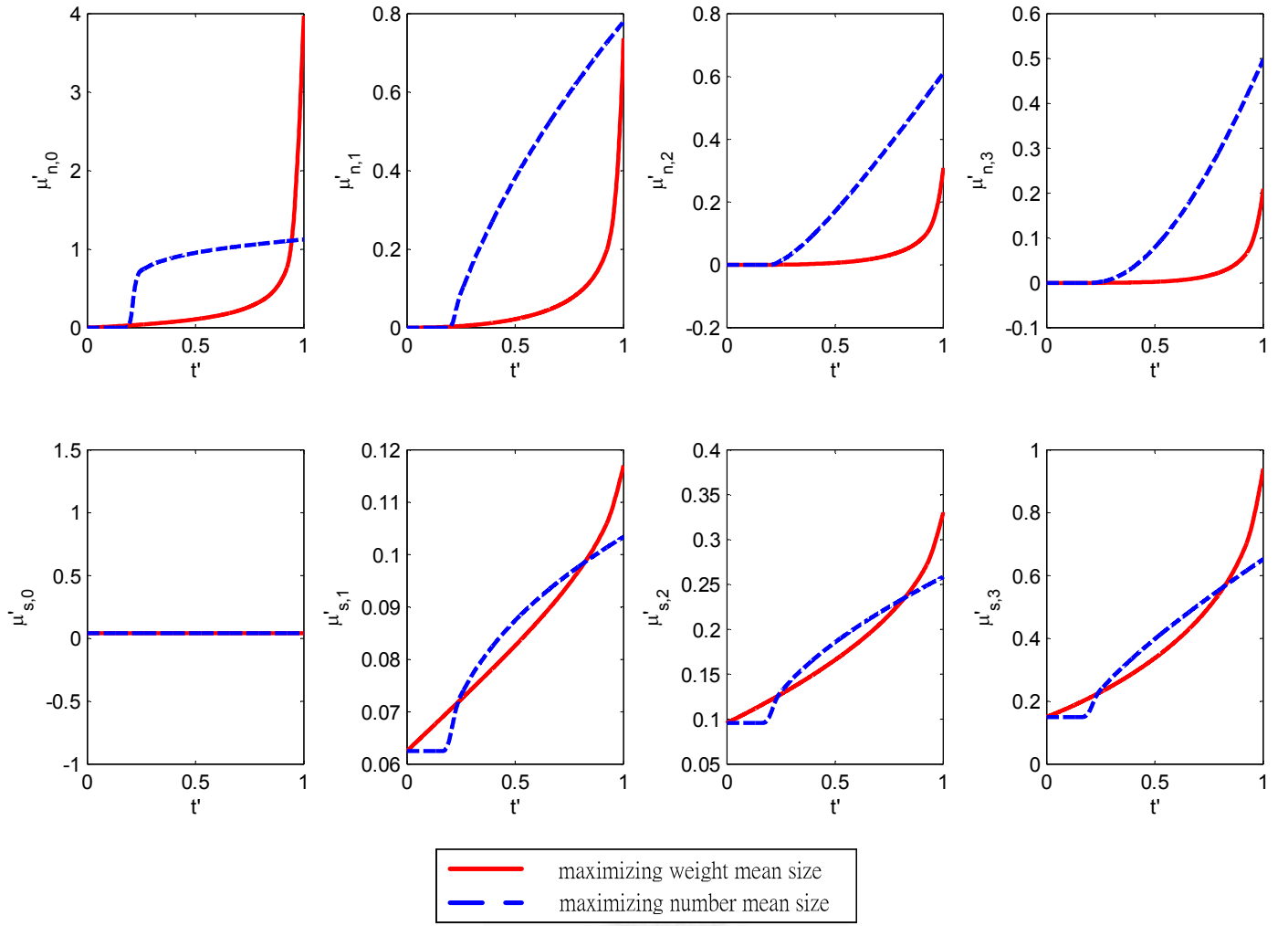


**Figure 15:** Different order of moment plot during the batch time for using objectives function minimizing weight mean size and minimizing number mean size.

We compare objectives involving maximizing a mean size of the final product crystals, either the weight mean size or number mean size. Figure 16 shows the results for maximizing the weight mean size and the number mean size. In Panel A, as expected, if the objective is to maximize the weight mean

size, then the product crystals do indeed have a larger weight mean size than if the objective is to maximize the number mean size. Likewise, from Panel B, if the objective is to maximize the number mean size then the resulting product crystals do indeed have a larger number mean size than if the objective is to maximize the weight mean size.



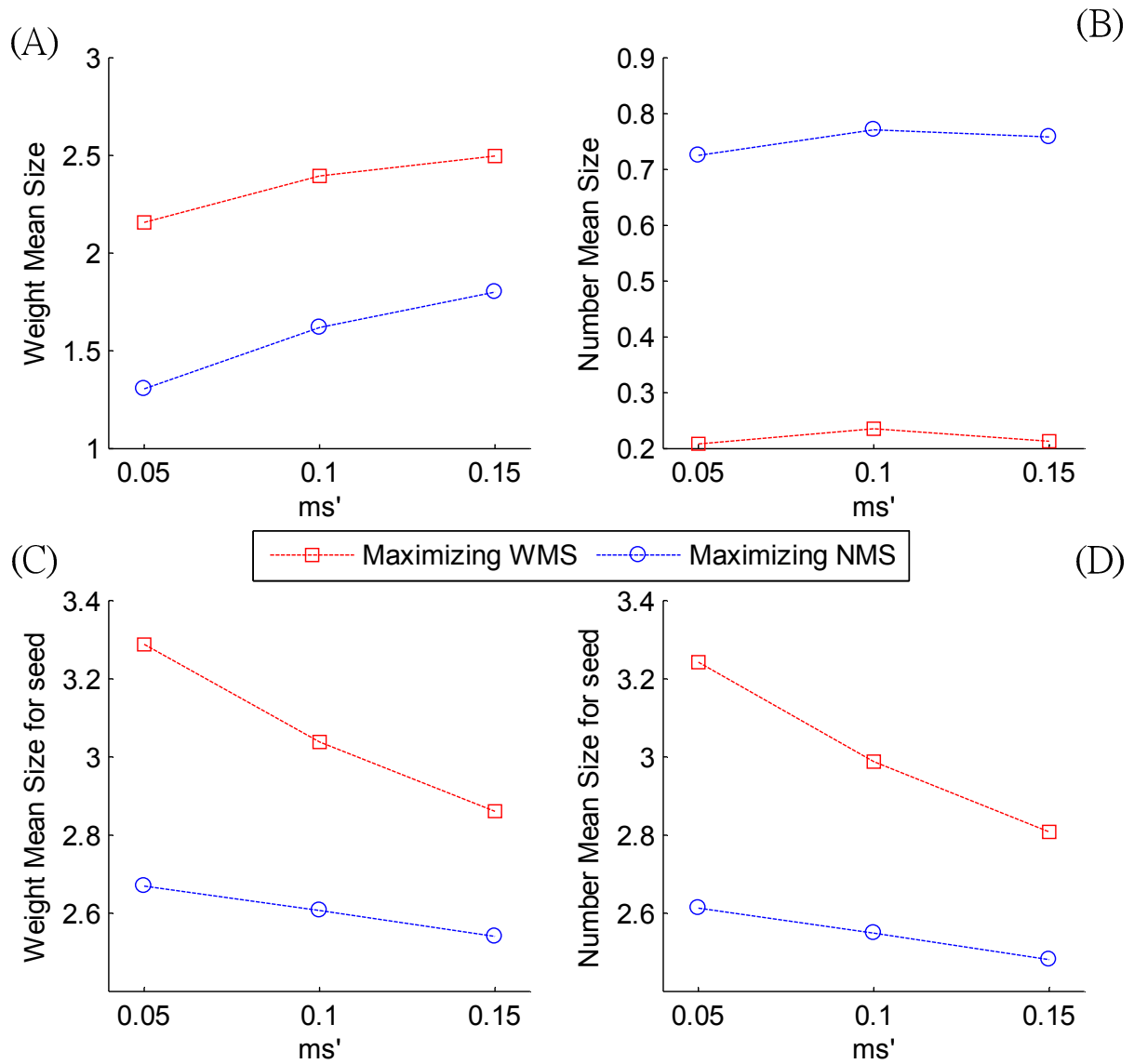


**Figure 16:** Weight mean size and number mean size value for different objectives.

However, as was the case for objectives based on COV, the situation changes if only the seed crystals are considered. (Panels C and D) In this case, maximizing the weight mean size gives a better result for both objectives.

Figure 17 shows the number distribution and weight distribution that result

from the saturation concentration trajectories determined using both objective functions. The objective of maximizing the weight mean size results in greater growth of the seed crystals. Therefore, among the two objective functions that involve product mean sizes, we conclude that weight mean size is a superior objective to number mean size.

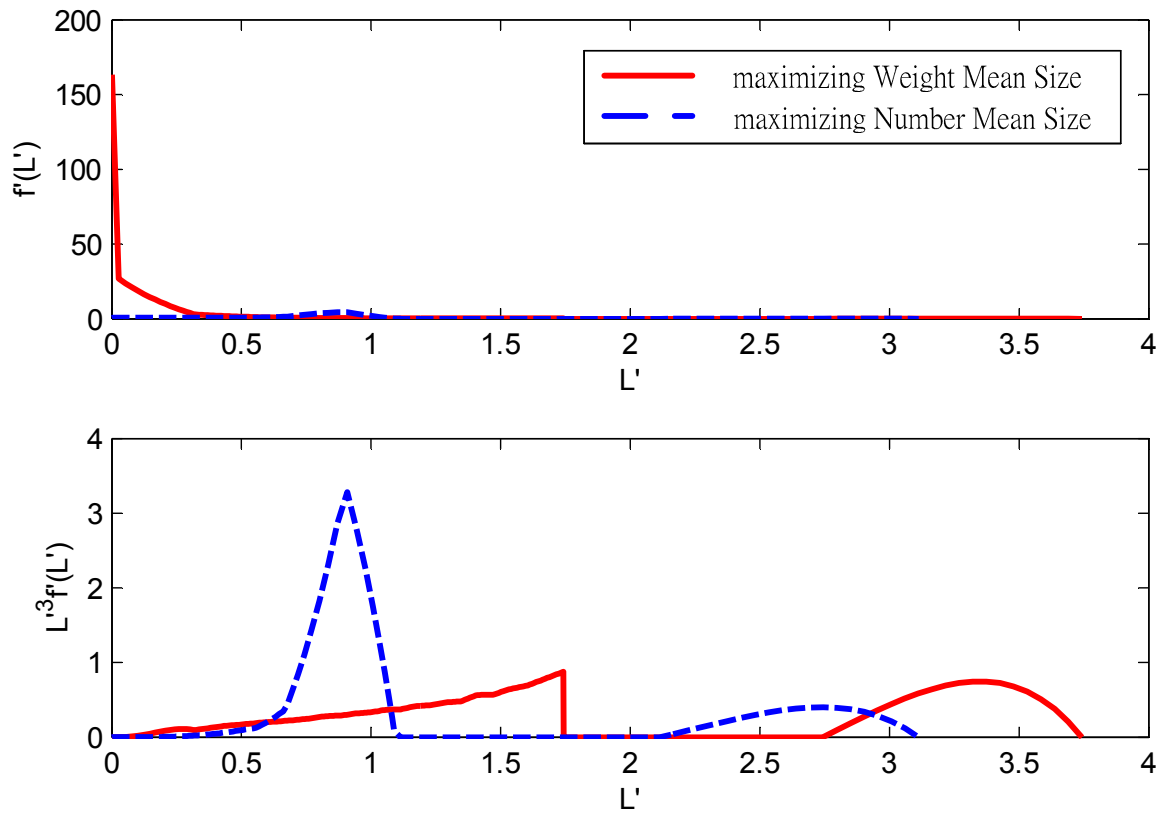


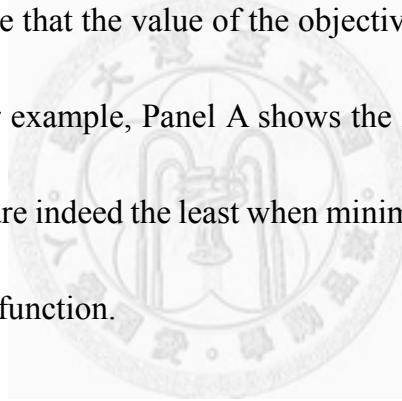
**Figure 17:** Final crystal size distribution for different objectives.



#### 4.5. Single Moment Objective Functions

Finally, we consider objectives that are based on minimizing a single moment of the nucleated crystals, that is minimizing  $\mu_{n0}$ ,  $\mu_{n1}$ ,  $\mu_{n2}$  and  $\mu_{n3}$ .

Figure 18 shows a comparison of the results. Each panel shows a different moment of the nucleated crystals at the end of the batch, and each line corresponds to the result that is obtained using the saturation concentration trajectory that minimizes a different moment. In each case, the optimization is successful in the sense that the value of the objective is always least when that objective is used. For example, Panel A shows the zeroth moment of the final CSD, and the values are indeed the least when minimizing the zeroth moment is used as the objective function.



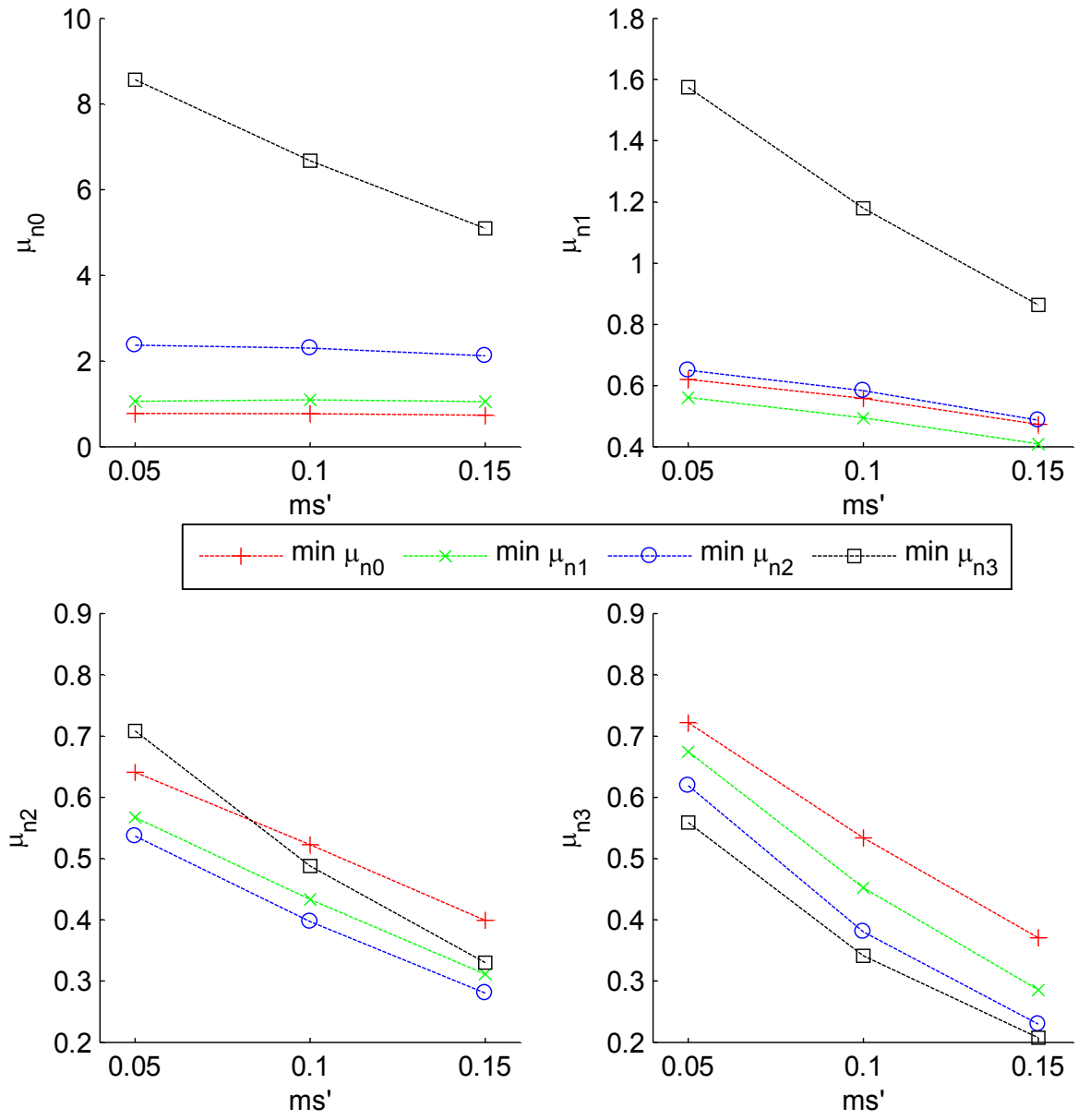


**Figure 18:** Nucleated crystal moments of for different objectives.

However, again the situation changes when only the seed crystals are considered (Fig. 19). In this case, the zeroth moment of the crystal size distribution is the same in all cases, because according to our assumptions no additional seeds can be formed during the batch. However, for the other moments, minimizing the third moment of the nucleated crystals maximizes all of the other moments (1-3) of the seed-grown crystals.

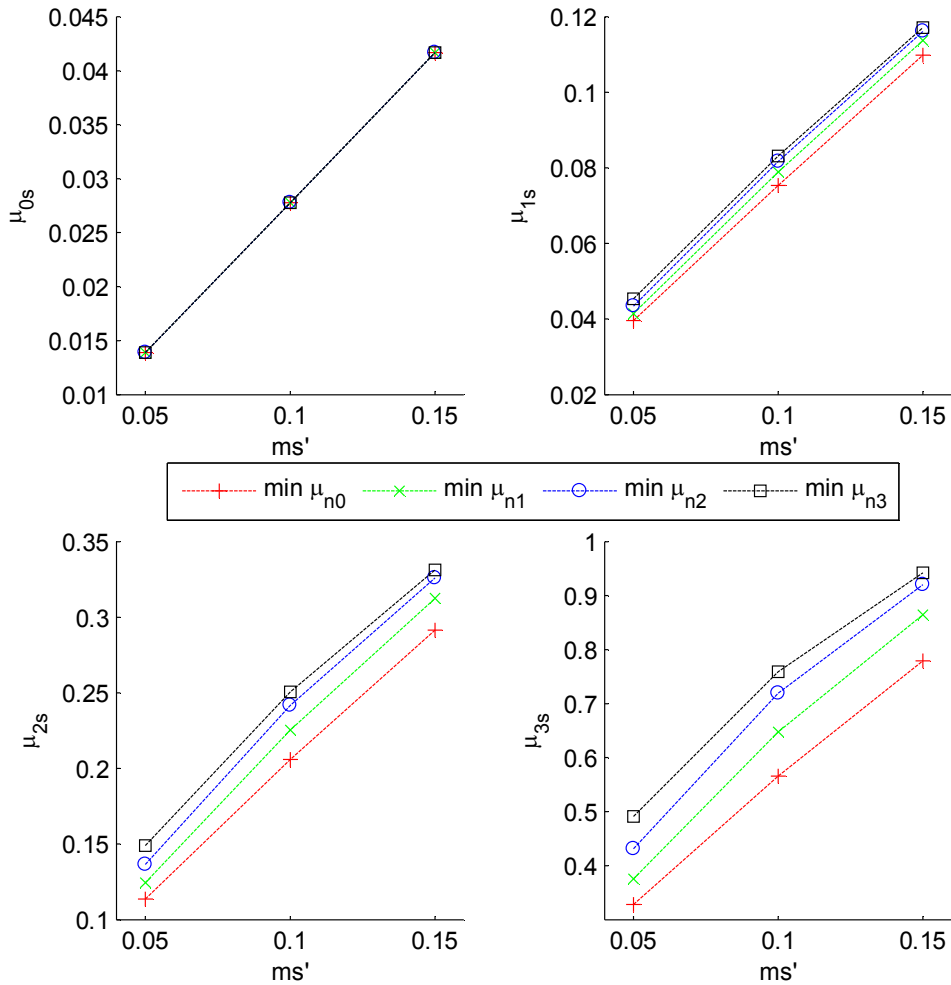


**Figure 19:** Seeded crystal moments for different objectives.

Figure 20 shows the number distribution and mass distribution that result from using the different objective functions. Minimizing the third moment of the nucleated crystals maximizes the growth of the seeds. Therefore, among objectives that are based on a single moment of the nuclei, minimizing the third moment of the nuclei seems to be the best.

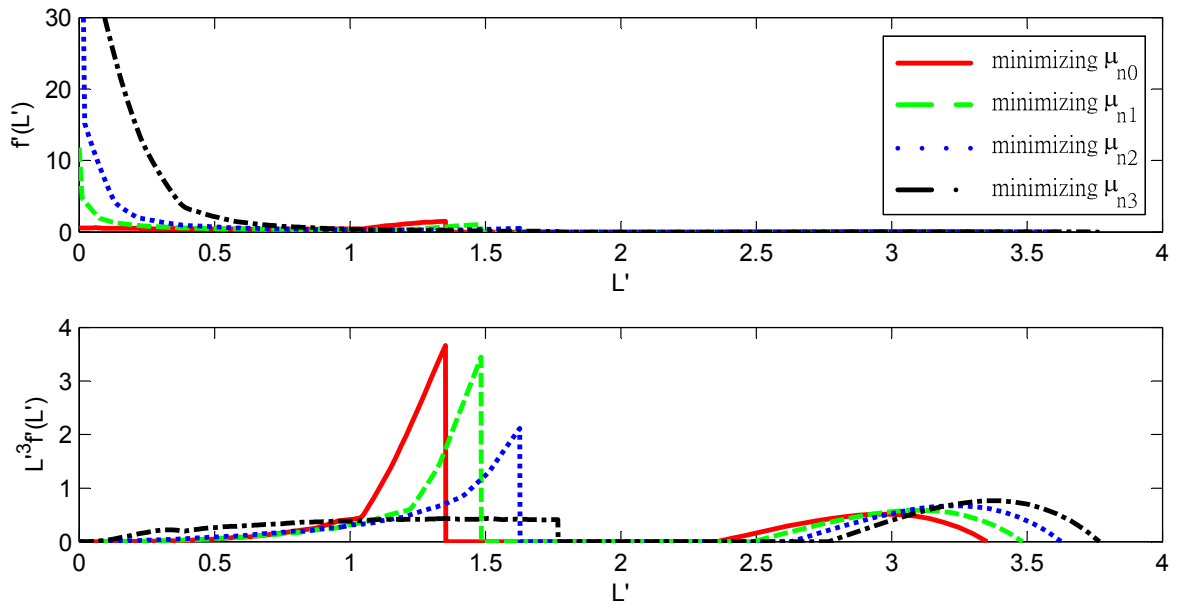


**Figure 20:** Final crystal size distribution for different objectives.

Figures 22 and 23 shows the optimal nucleation rate and optimal growth rate trajectory using minimizing  $\mu_{n0}$ ,  $\mu_{n1}$ ,  $\mu_{n2}$  and  $\mu_{n3}$  as objective functions. The optimal trajectory minimizing  $\mu_{n0}$  is an early growth trajectory because in Equation 26  $\mu_{n0}$  is directly affect by the nucleation rate which is affected by the third moment of the crystals. Since the third moment of the crystal is

constantly increasing during the batch, it is desirable to assign more supersaturation at the beginning of the batch instead of at the end of the batch, where large value of  $\mu_3$  would enhance the nucleation. From Equation 26 to Equation 29, increase of  $\mu_0$  eventually causes an increase in  $\mu_1$ , and an increase of  $\mu_1$  causes an increase of  $\mu_2$ , and so on. From these relationships we know that when the supersaturation increases,  $\mu_0$  will increase first (before the other moments) because it is directly related to the nucleation rate, and then  $\mu_1$ ,  $\mu_2$  and finally  $\mu_3$ . Late growth trajectory is desirable for the objective function minimizing the  $\mu_{n3}$  for of two reason. One is that if the nucleation is suppressed all the time except the end of the batch, only small amount of nucleated crystals would compete with seed crystal for the mass of the solute in the solvent. Another reason is that even if the nucleation rate is very large at the end of the batch, the third moment reacts slowly. The process ends before the  $\mu_{n3}$  gets large. The optimal trajectory for minimizing  $\mu_{n1}$  and  $\mu_{n2}$  is “in between” the optimal trajectory for minimizing  $\mu_{n0}$  and  $\mu_{n3}$ .

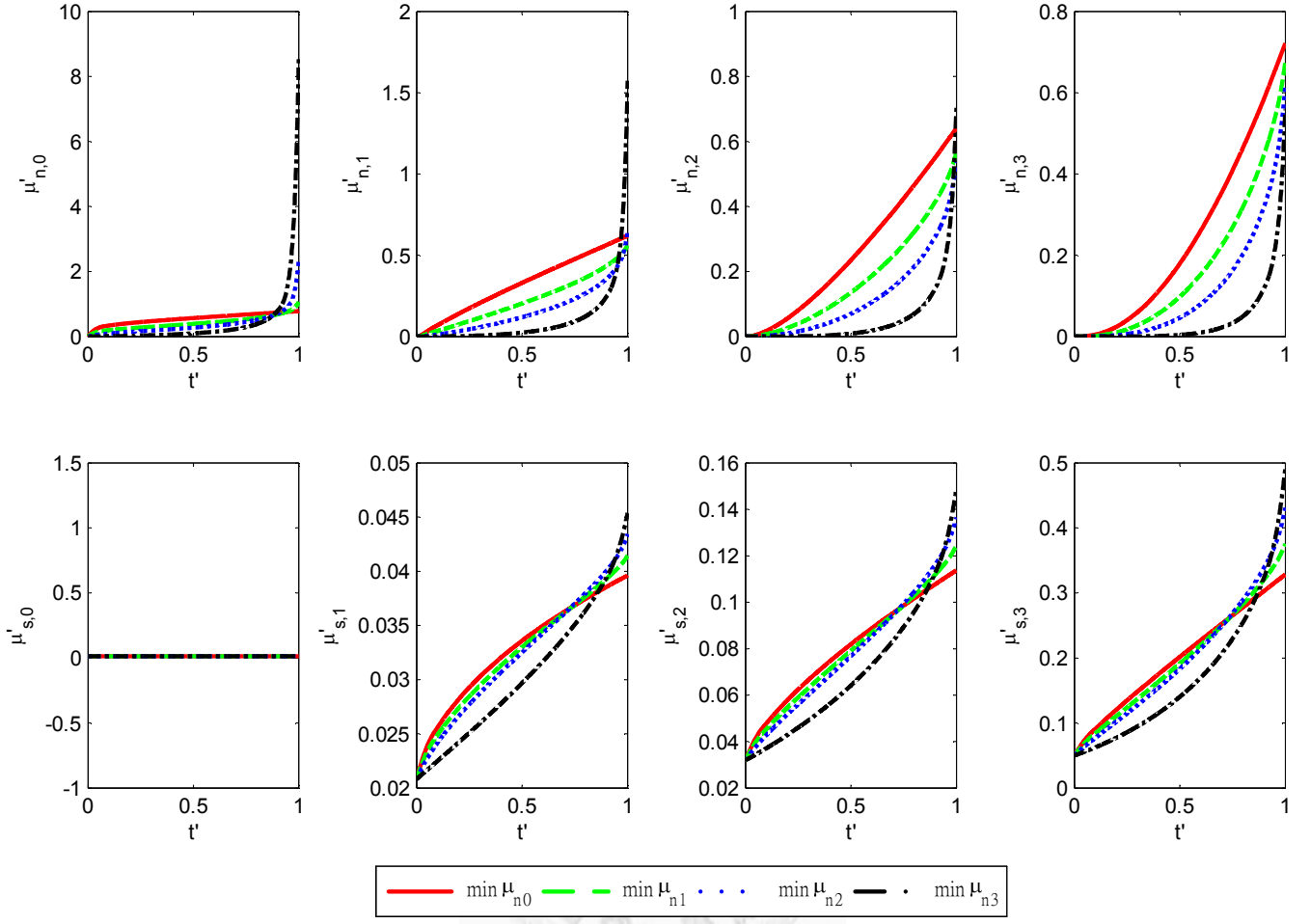


**Figure 21:** Different order of moments during the batch using minimizing  $\mu_{n0}$ ,

$\mu_{n1}$ ,  $\mu_{n2}$  and  $\mu_{n3}$  as objective function.

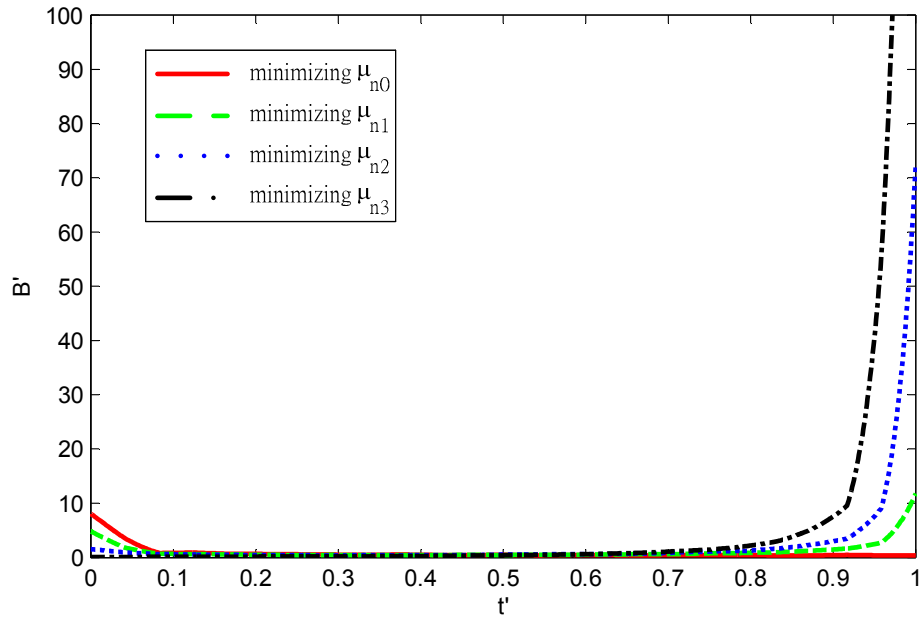


**Figure 22:** The optimal nucleation rate trajectory using minimizing  $\mu_{n0}$ ,  $\mu_{n1}$ ,  $\mu_{n2}$  and  $\mu_{n3}$  as objective function.

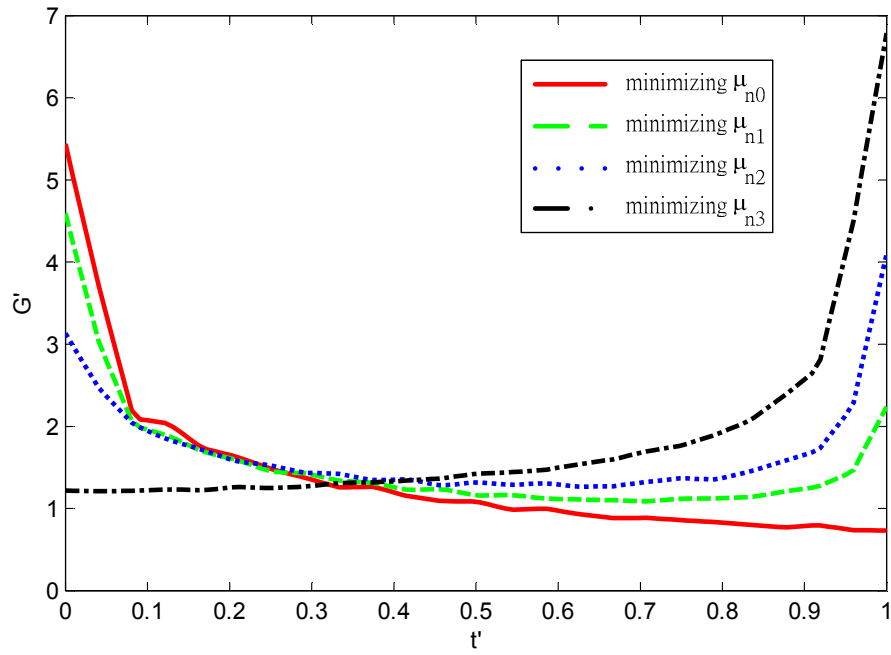
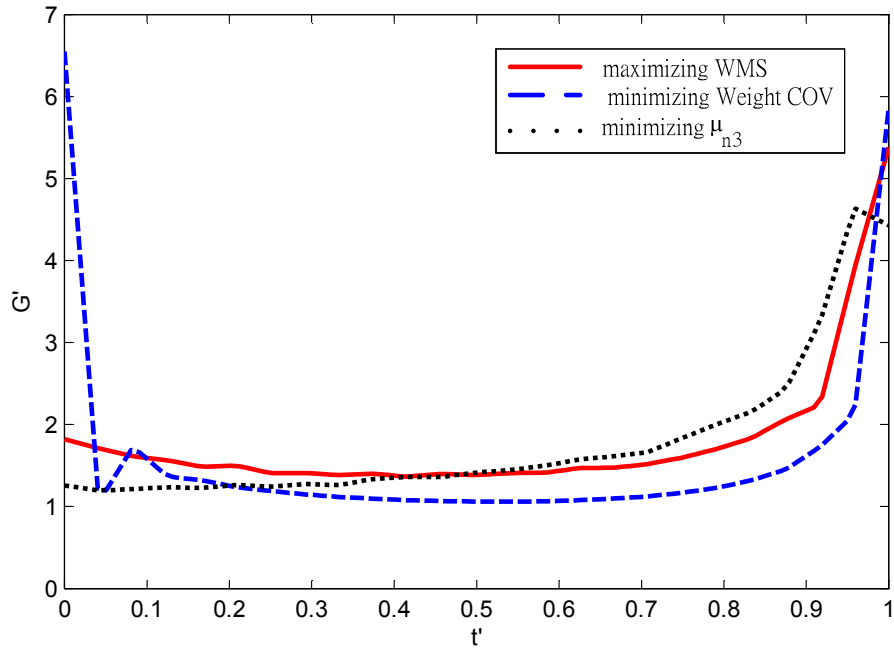


**Figure 23:** The optimal growth rate trajectory using minimizing  $\mu_{n0}$ ,  $\mu_{n1}$ ,  $\mu_{n2}$  and  $\mu_{n3}$  as objective function.

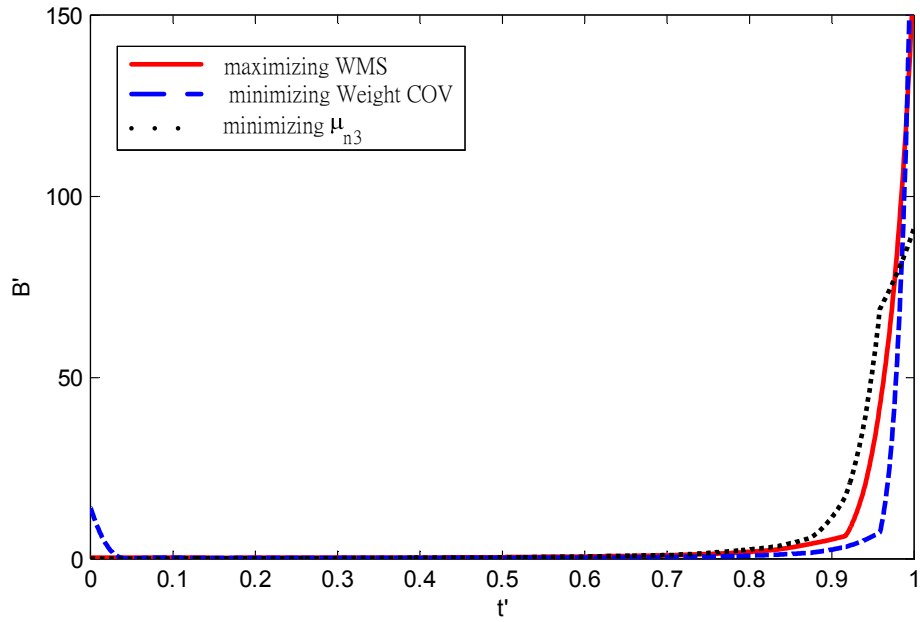
#### 4.6. Objective Function Category Comparison

Finally, we compare the best result from each of the three categories of objective functions to see which is the best overall. Figure 24 shows the growth rate trajectory for objective function “maximizing weight mean size,” “minimizing weight coefficient of variation” and “minimizing  $\mu'_{3n}$ .” It shows that all of the result have high growth rate at the end of the batch. The major difference is at the beginning of the batch that the result from using objective function “minimizing weight coefficient of variation” launch a large supersaturation. This can be also observed from Figure 25. For these three result from different objective function, only the result using objective function “minimizing weight coefficient of variation” has a peak at the beginning of the batch in Figure 25.

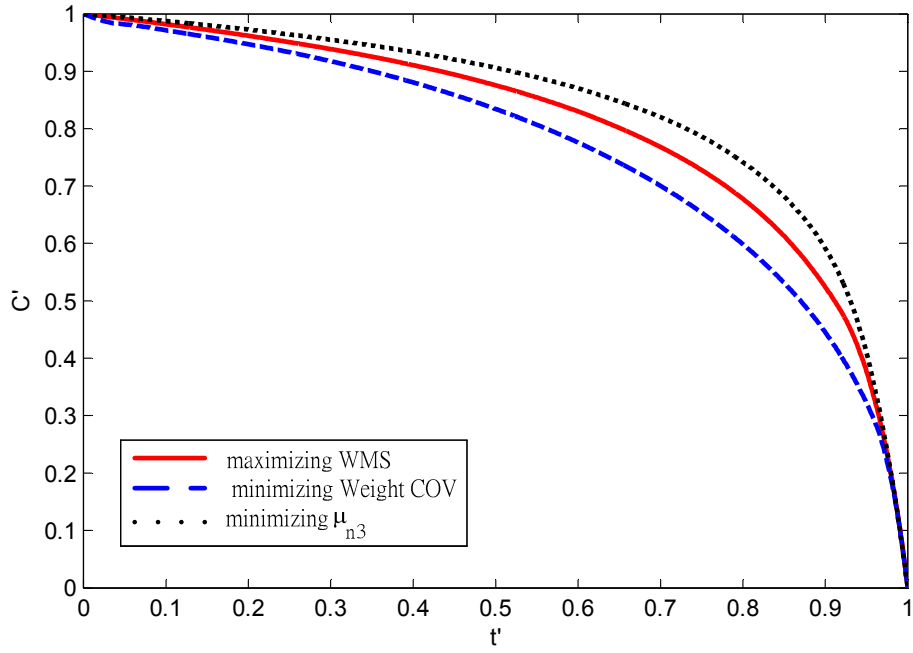




**Figure 24:** The optimal growth trajectory using minimizing  $\mu_{n3}$ , weight coefficient of variation and maximizing weight mean size.



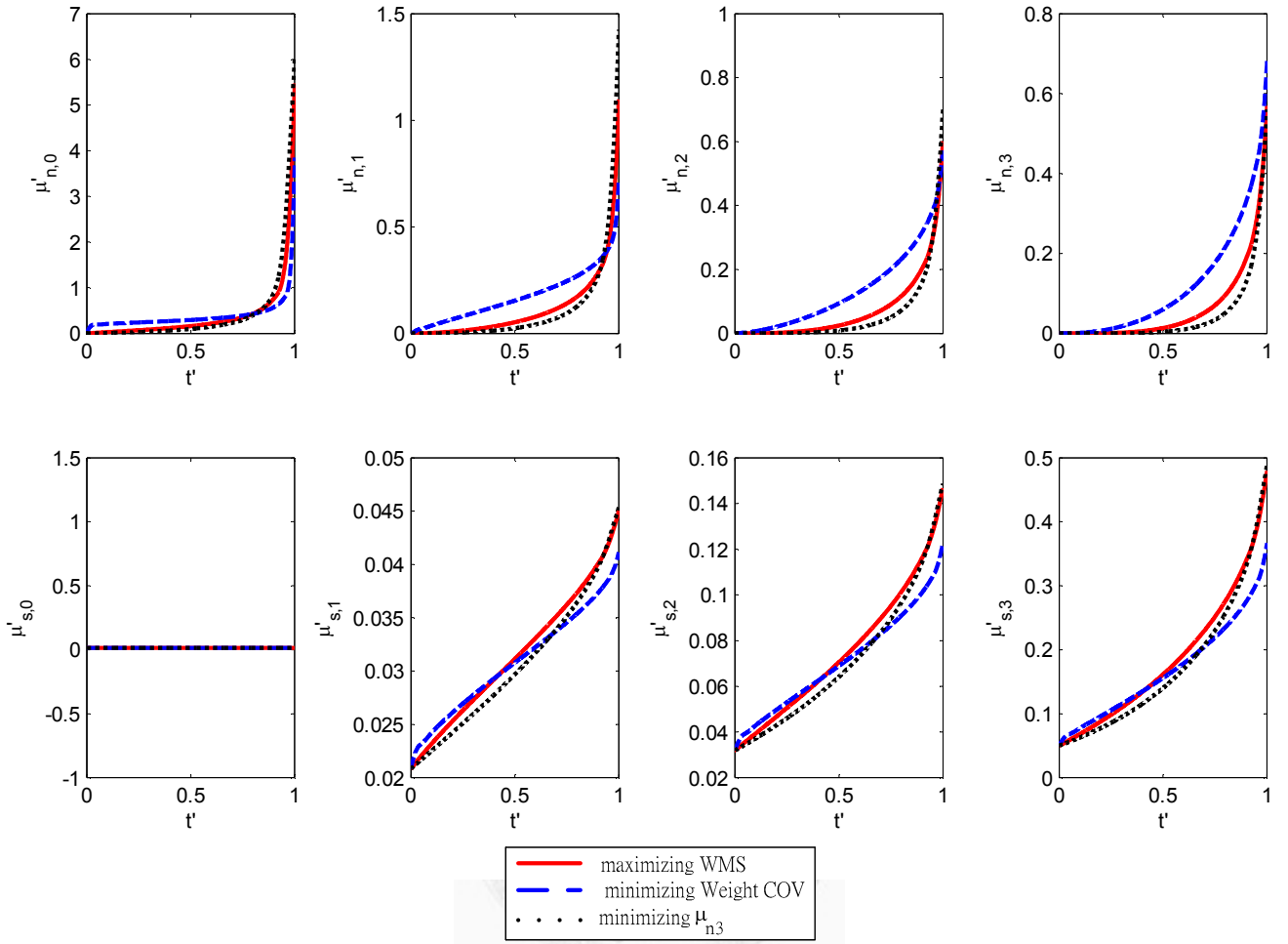
**Figure 25:** The optimal nucleated trajectory using minimizing  $\mu_{n3}$ , weight coefficient of variation and maximizing weight mean size.



**Figure 26:** The optimal concentration trajectory using minimizing  $\mu_{n3}$ , weight coefficient of variation and maximizing weight mean size.

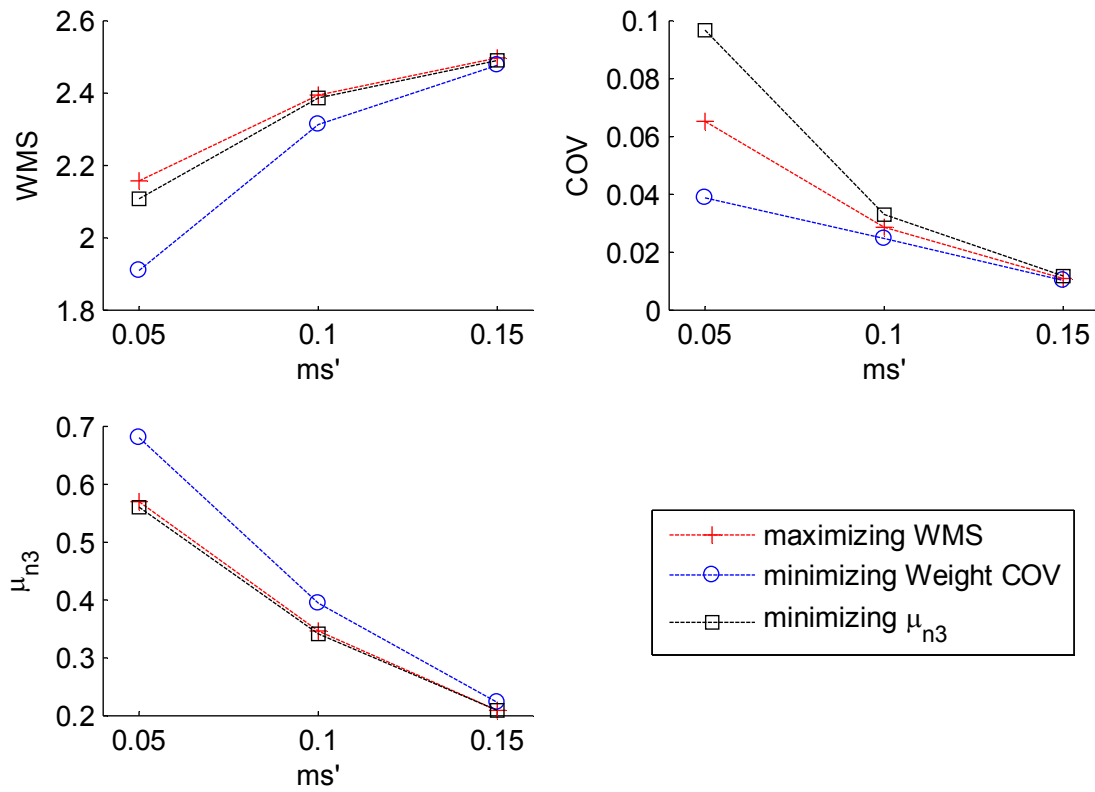
Figure 26 shows the concentration trajectory using three objective functions. We can observe that the trajectory from using objective function “minimizing weight coefficient of variation” is more like linear trajectory.

Figure 27 shows different moment during the batch. The upper panels represent the nucleated crystals, we can observe that the moment of nucleated crystal from objective function “minimizing weight coefficient of variation” is higher than others at most of the batch time. The lower panels shows the seeded crystal moments. At the end of the batch, the result from objective function “minimizing  $\mu'_{3n}$ ” is larger than others at the end of the batch.



**Figure 27:** Different moments during the batch using minimizing  $\mu_{n3}$ , weight coefficient of variation and maximizing weight mean size.

Figure 28 shows the results. As before, the trajectory determined using each objective function performs the best according to the standard of that objective. However, again the situation changes when only the seed properties are considered. In this case, minimizing  $\mu_{n3}$  always performs the best, although the result is similar to the result for maximizing the WMS.



**Figure 28:** Weight mean size, weight coefficient of variation and third moment values for different objectives.

Figure 29 shows the number distribution and mass distribution that result from using the three objectives. Maximizing WMS and minimizing  $\mu_{n3}$

perform similarly, but minimizing  $\mu_{n3}$  is slightly better. Therefore we consider that minimizing  $\mu_{n3}$  is the best overall.

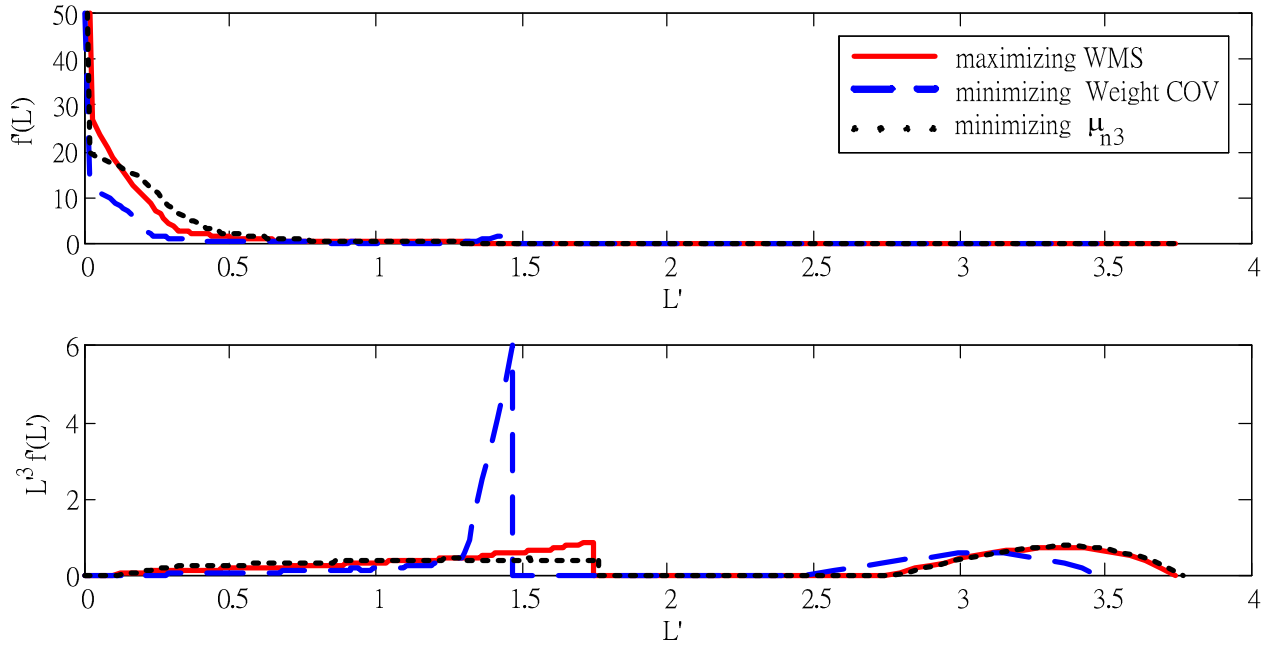


**Figure 29:** Final crystal size distribution for different objectives.

Minimizing  $\mu_{n3}$  also has an especially simple physical interpretation. It simply means that the seeds are grown as large as possible, that is as much mass as possible is transferred to the seeds and as little mass as possible is consumed by the formation and growth of nuclei.

#### 4.7. Other Solution For Minimizing Coefficient of variation

In many cases, it may be desired that the product crystals have a distribution with some desired properties, such as a narrow width. It may be tempting to try to achieve this result by formulating it into an objective function and seeking out a cooling trajectory that minimizes the objective. However, we feel that such an objective can be achieved much more easily by manipulating the seed crystal size distribution rather than by adjusting the cooling trajectory. For example, if product crystals with a narrow size distribution are desired, then one should start with seeds with a narrow distribution, and grow them to a larger size. If a distribution with some other shape, such as rectangular or trapezoidal, is desired, one should start with a seed distribution in this shape and then grow all of the seeds to a larger size. We feel that this approach is both more straightforward and more practical. If one uses an objective other than minimizing  $\mu_{n3}$ , one is in effect deliberately causing extra nucleation in the hopes that the nucleated crystals will somehow combine together with the seed crystals to improve the overall distribution. This is unlikely to be as effective as manipulating the seed distribution to obtain the desired product distribution, using a sufficient mass of seeds to suppress nucleation, growing the seeds as large as possible, and then filtering out any nuclei that do form.

To illustrate this, we calculated the saturation concentration trajectory that minimized the product weight coefficient of variation starting with seed distributions of different width, as shown in Figure 30. We illustrate different seed loading mass by different line color.

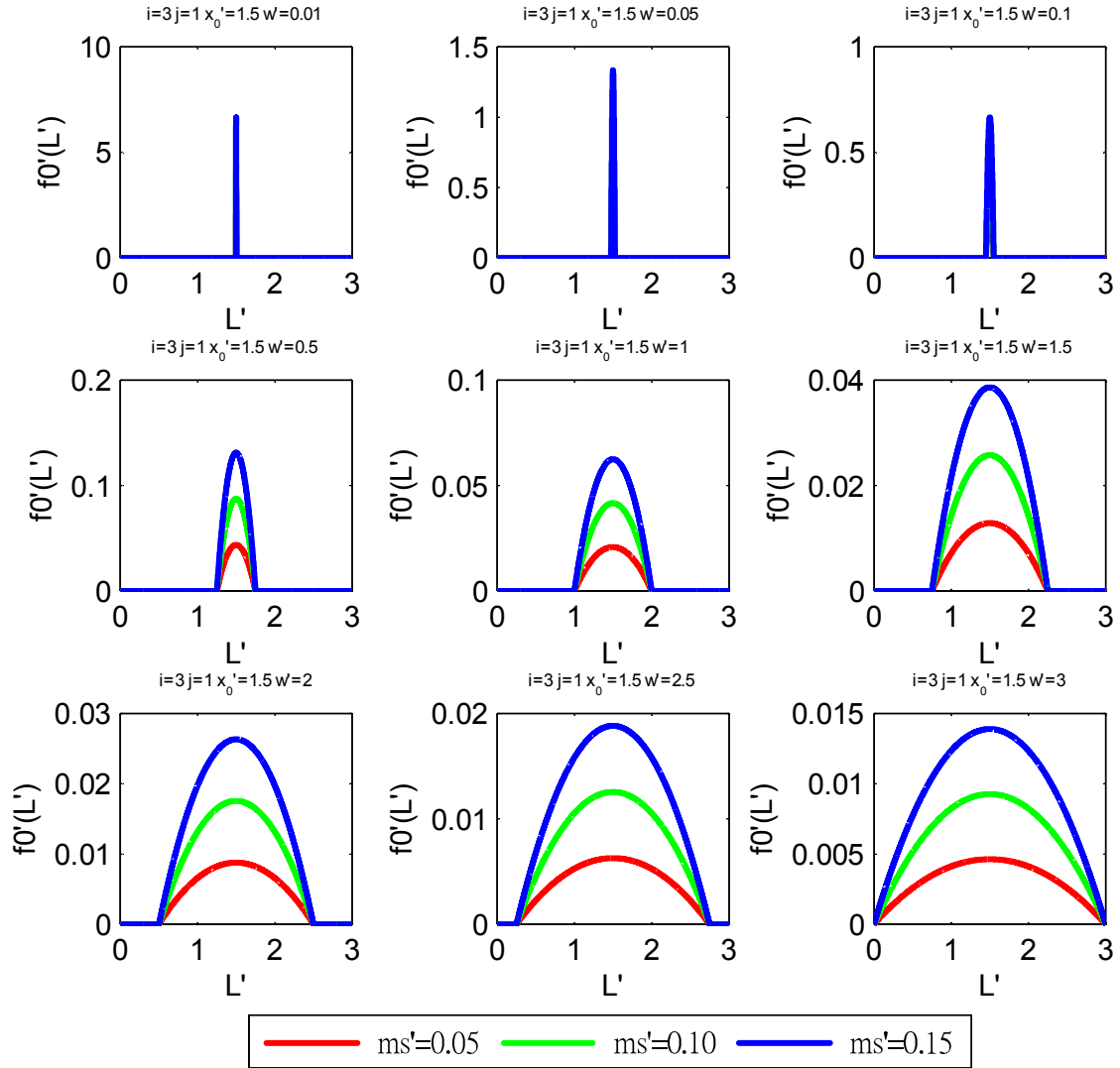


**Figure 30:** Initial crystal size distribution which is used for minimizing weight coefficient of variation result.

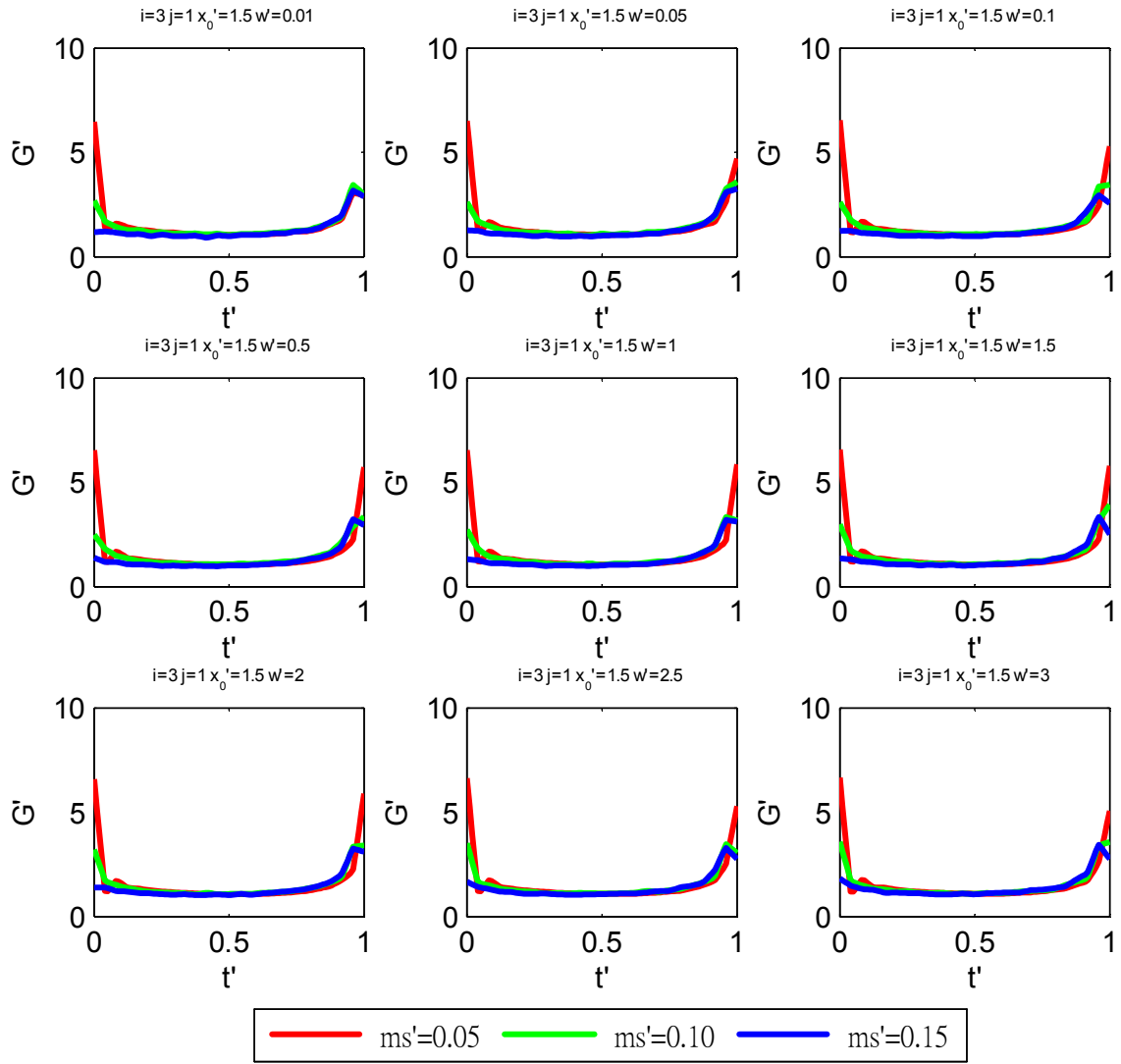


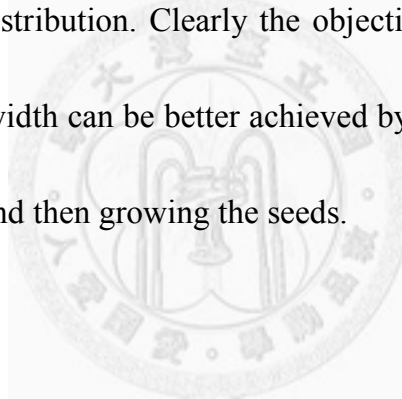
**Figure 31:** The growth trajectory for different seed distribution width which is used for minimizing weight coefficient of variation result.

The growth rate trajectory is shown in Figure 31. We can see that there is more excess nucleation for the system which is with wider seed distribution and less seed loading. One reason for this is that more seed loading is actually suppresses the nucleation. Another reason is that from Figure 30, initial seed



distribution for higher  $m'_s$  is relative narrow than seed distribution with less  $m'_s$  value.

The results are shown in Figure 32. If the seed width is narrow, then the trajectory that minimizes the weight COV will grow the seeds to a large size with little nucleation. However, as the width of the seed distribution increases, the objective is satisfied increasingly by producing a large amount of nuclei with a narrow distribution and then growing the nuclei. The result is an undesired bimodal distribution. Clearly the objective of producing a product CSD with a narrow width can be better achieved by starting with seeds with a narrow distribution and then growing the seeds.



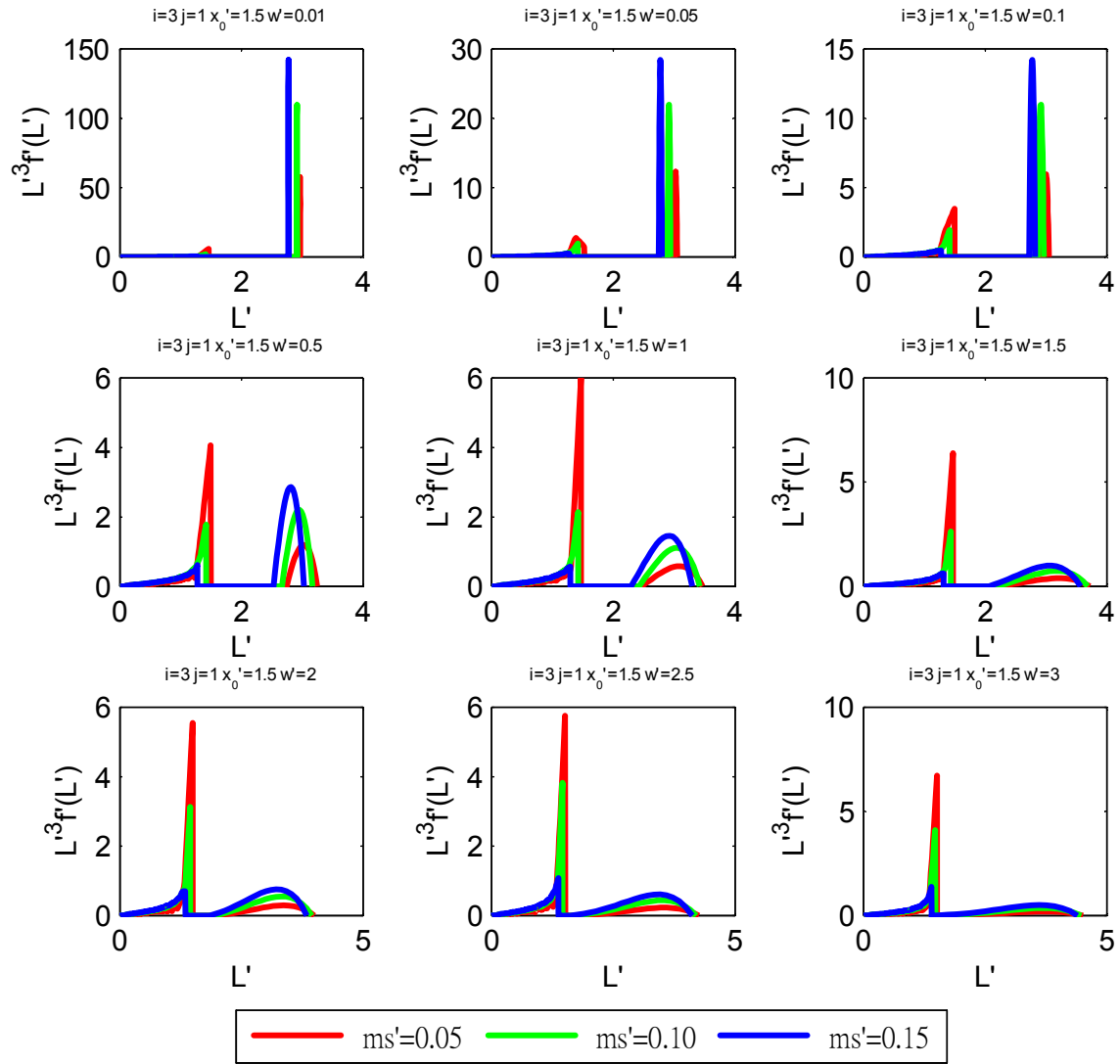


**Figure 32:** Final crystal size distribution for minimizing weight coefficient of variation.

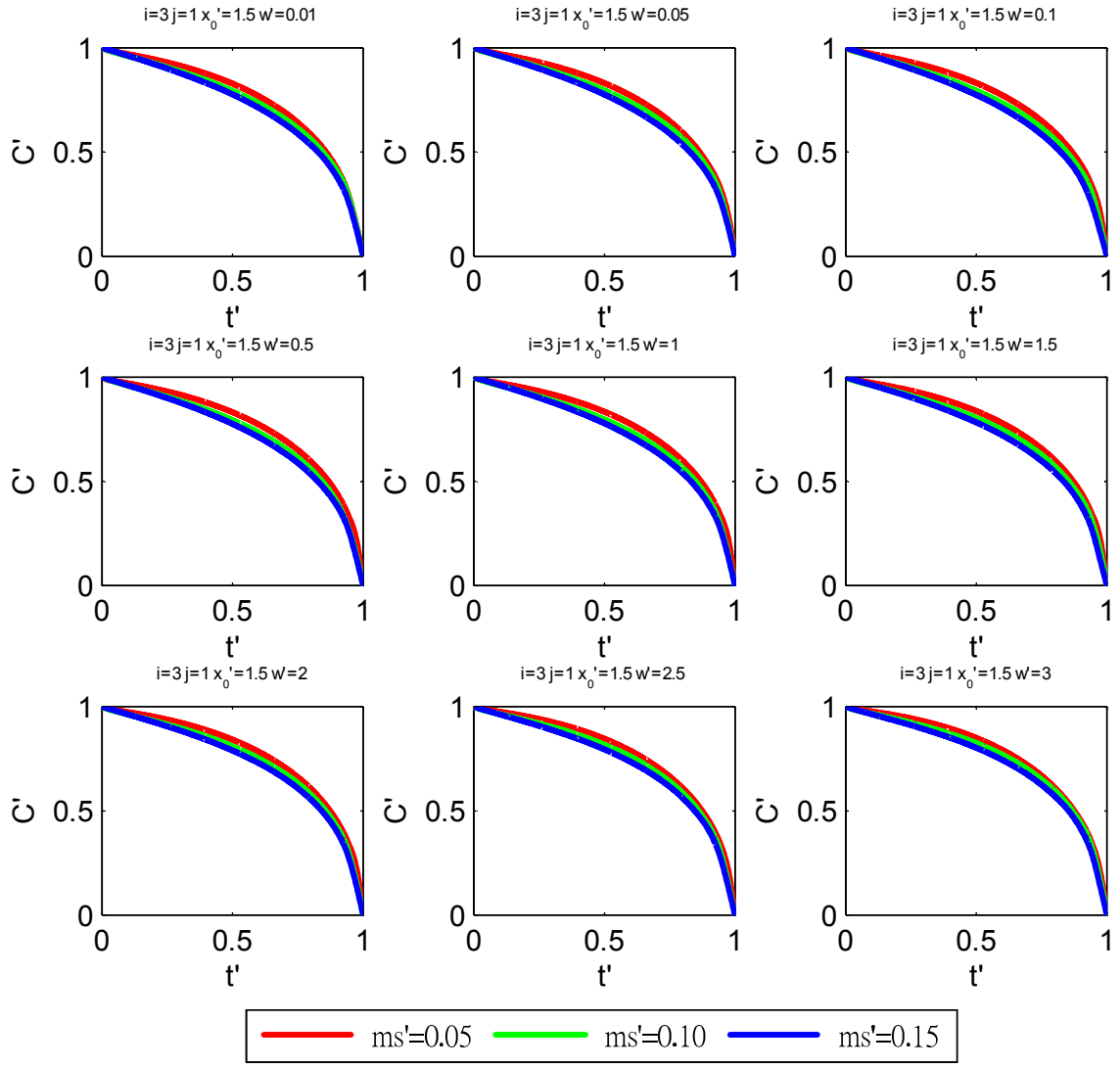


**Figure 33:** The concentration trajectory for different seed distribution width which is used for minimizing weight coefficient of variation result.

#### 4.8. The Effect of Changing j

It is known that the nucleation is not only related to the supersaturation, but also the crystal in the batch crystallizer. In our previous work, we only considered the situation that the exponent on the third moment in Equation 13 was equal to one. In this section, we discuss the situation that this exponent may change. The equation will be like this:

$$B = k_b G^\gamma \mu_3^j \quad (49)$$

Since the form of the expression for  $B$  changes, the unit of  $k_b$  also changes.

$$k_b [=] \frac{\#}{m^3 s} \left( \frac{m}{s} \right)^{-\gamma} \left( \frac{m^3 \text{crystals}}{m^3 \text{solution}} \right)^{-j} \quad (50)$$

The dimensionless third moment remains the same:

$$\bar{\mu}_3 = \frac{C_0^\dagger}{\rho_c k_v} = \frac{(C_0 - C_f)}{\rho_c k_v} \quad (51)$$

Define

$$\bar{\mu}_0 = \bar{B} t_f \quad (52)$$

$$\bar{\mu}_1 = \bar{B} \bar{G} t_f^2 \quad (53)$$

$$\bar{\mu}_2 = \bar{B} \bar{G}^2 t_f^3 \quad (54)$$

$$\bar{\mu}_3 = \bar{B} \bar{G}^3 t_f^4 \quad (55)$$

We want the dimensionless moments ODE set would be like this:

$$\frac{d\mu'_0}{dt} = B' = (G')^\gamma \mu_3'^j \quad (56)$$

$$\frac{d\mu'_1}{dt} = G' \mu'_0 \quad (57)$$

$$\frac{d\mu'_2}{dt} = 2G' \mu'_1 \quad (58)$$

$$\frac{d\mu'_3}{dt} = 3G' \mu'_2 \quad (59)$$

Therefore, we define

$$\bar{G} = (k_b \bar{\mu}_3^{j-1} t_f^4)^{\frac{-1}{\gamma+3}} \quad (60)$$

$$\bar{B} = k_b \bar{\mu}_3^j (k_b t_f^4)^{\frac{-\gamma}{\gamma+3}} \quad (61)$$

The dimensionless crystal birth and crystal growth becomes

$$B' = \frac{B}{\bar{B}} = \frac{B}{k_b \bar{\mu}_3^j (k_b t_f^4)^{\frac{-\gamma}{\gamma+3}}} \quad (62)$$

$$G' = \frac{G}{\bar{G}} = \frac{G}{(k_b \bar{\mu}_3^{j-1} t_f^4)^{\frac{-1}{\gamma+3}}} \quad (63)$$

Note that

$$\bar{B} \bar{G}^3 t_f^4 = k_b \bar{\mu}_3^j (k_b \bar{\mu}_3^{j-1} t_f^4)^{\frac{-\gamma}{\gamma+3}} (k_b \bar{\mu}_3^{j-1} t_f^4)^{\frac{-3}{\gamma+3}} t_f^4 = \bar{\mu}_3 \quad (64)$$

Define

$$f'(L) = \frac{\bar{G} f(L)}{\bar{B}} \quad (65)$$

The dimensionless initial seed crystal size distribution becomes:

$$f'(L) = -\frac{\bar{G} m_s}{\bar{B} (\bar{G} t_f)^4 \rho k_v} \left( \frac{1}{6} x_0'^3 w'^3 + \frac{1}{40} x_0' w'^5 \right)^{-1} \left( L' - \left( x_0' - \frac{w'}{2} \right) \right) \left( L' - \left( x_0' + \frac{w'}{2} \right) \right) \quad (66)$$

Applying Equations 61 and 60 we have:

$$f'(L) = -\frac{m_s}{\bar{\mu}_3 \rho k_v} \left( \frac{1}{6} x_0'^3 w'^3 + \frac{1}{40} x_0' w'^5 \right)^{-1} \left( L' - \left( x_0' - \frac{w'}{2} \right) \right) \left( L' - \left( x_0' + \frac{w'}{2} \right) \right) \quad (67)$$

with Equation 51, the equation becomes:

$$f'(L) = -m'_s \left( \frac{1}{6} x_0'^3 w'^3 + \frac{1}{40} x_0' w'^5 \right)^{-1} \left( L' - \left( x_0' - \frac{w'}{2} \right) \right) \left( L' - \left( x_0' + \frac{w'}{2} \right) \right) \quad (68)$$

Where the parameter of seed distribution function are defined as:

$$m'_s = \frac{m_s}{C_0^\dagger} \quad (69)$$

$$x_0' = \frac{x_0}{\bar{G} t_f} \quad (70)$$

$$w' = \frac{w}{\bar{G} t_f} \quad (71)$$

The dimensionless average size of the seed for j and j=1 are:

$$x_0' \Big|_j = \frac{x_0}{\bar{G} t_f} = \frac{x_0}{\left( k_b t_f^4 \right)^{\frac{-1}{\gamma+3}} t_f} \quad (72)$$

$$x_0' \Big|_{j=1} = \frac{x_0}{\bar{G} t_f} = \frac{x_0}{\left( k_b \bar{\mu}_3^{j-1} t_f^4 \right)^{\frac{-1}{\gamma+3}} t_f} \quad (73)$$

Divide the above equations we have:

$$x_0' \Big|_j = x_0' \Big|_{j=1} \times \bar{\mu}_3^{\frac{1-j}{\gamma+3}} \quad (74)$$

This is the new dimensionless average size of the seed for j value that is

not one. Similarly we have the dimensionless seed distribution width:

$$w_0' \Big|_j = \frac{w_0'}{\bar{G} t_f} = \frac{w_0'}{\left( k_b t_f^4 \right)^{\frac{-1}{\gamma+3}} t_f} \quad (75)$$

$$w'_0 \Big|_{j=1} = \frac{w'_0}{\overline{G} t_f} = \frac{w'_0}{\left(k_b \bar{\mu}_3^{j-1} t_f^4\right)^{\frac{-1}{\gamma+3}} t_f} \quad (76)$$

Divide the above equations we have:

$$w'_0 \Big|_j = w'_0 \Big|_{j=1} \times \bar{\mu}_3^{\frac{1-j}{\gamma+3}} \quad (77)$$

Changing the variable  $j$  will also cause the shift of the dimensionless seed distribution average and width. However, the shifting is depends on  $\bar{\mu}_3$ , and it is depends on the chemicals. In this work, we consider the case where  $\bar{\mu}_3$  is equal to one.

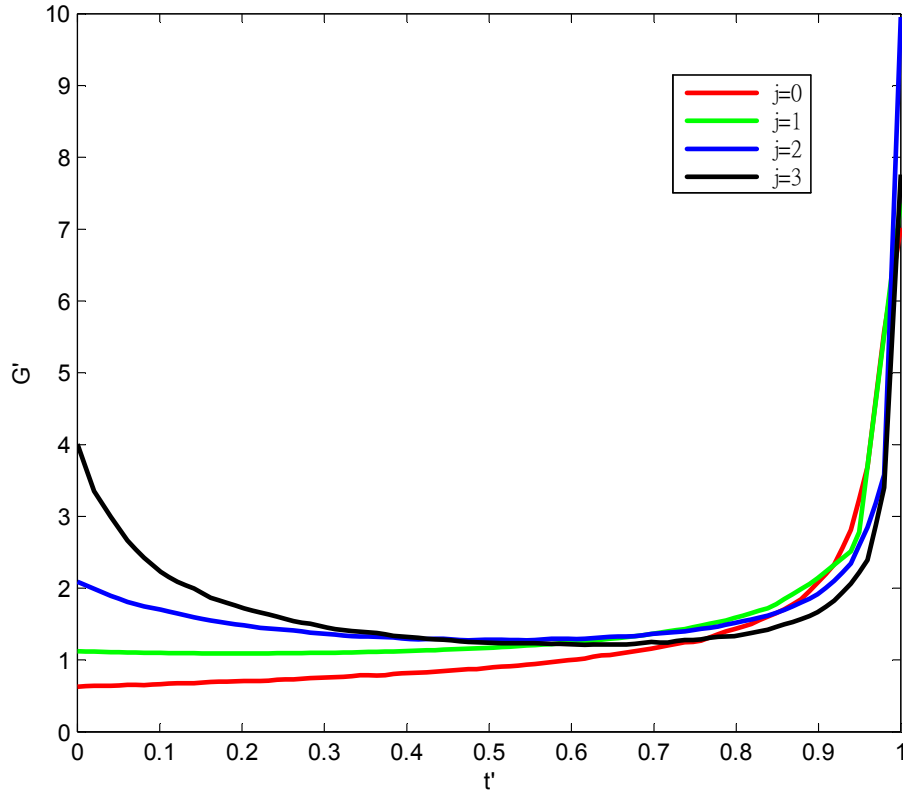


**Figure 34:** The growth rate for different  $j$ .

We optimize using the objective “minimizing  $\mu'_{3n}$ ”, From Figure 34, optimized trajectory for different  $j$  value both tend to have high growth rate late in the batch. The major reason is that if the growth rate or supersaturation rises, the nucleation rate will rise larger than growth rate. And to achieve the goal of final production mass, the area under the growth rate trajectory has to be some fixed value. The question becomes that is it better to put more under line area at the beginning of the batch, or at the end of the batch.

It is also known that the third moment of the crystal will react slower than lower level of moments after the growth rate trajectory raises. Although using this late growth trajectory will cause large amount of the nuclei forms at the end of the batch, there is no time for them to grow up to enough mass that affects the objective function value. Therefore for objective function that minimizes the third moment of the nucleated crystal, the optimal growth trajectory is tending to be a late growth trajectory.

The major difference of the optimized growth trajectory is at the beginning of the batch. We can see that in Figure 34, optimal trajectory for  $j$  equal to zero tend to lower value at the beginning of the batch. For  $j$  equal to one the optimal growth trajectory is slightly higher than trajectory that for  $j$



equal to zero. For  $j$  equal to three, the beginning value of the optimal growth trajectory is the highest.

It is known that the nucleation rate is not related to the crystal amount in the batch crystallizer if the  $j$  equal to zero. This idea comes from Equation 49, when the  $j$  equal to zero, the nucleation rate becomes:

$$B = k_b G^\gamma \quad (78)$$

There is no third moment term in the equation, so the nucleation rate is no longer related to the third moment of the crystals. Since the nucleation rate is only depends on the supersaturation, then the optimal trajectory for minimizing the mass of the nucleated crystal tend to have small supersaturation during the batch, and have large supersaturation at the end of the batch such that even nucleation happens, there's no time for nucleated crystals to growth.

For  $j$  not equal to zero, this is the value widely used for crystallization process. The nucleation rate is related to both the supersaturation and the mass of the crystal in the batch crystallizer. If there's more crystals in the batch crystallizer, the nucleation increase. Then it comes to the problem that where to put more area under the growth trajectory line. To minimize the mass of the nucleated crystals, one strategy is to set higher supersaturation at both the beginning and the end of the batch. The advantage that put more growth rate or

higher supersaturation at the end of the batch is the same for the  $j$  equal to zero. That is there is not time for newly formed nucleated crystals to accumulate enough mass. And there is also an advantage to set the supersaturation to a higher value at the beginning of the batch compared to the middle of the batch. The total mass of crystals is always increasing during the batch process. Therefore for the same value of supersaturation, at the beginning of the batch there will be less nucleation than at the middle of the batch. So the optimal trajectory tends to have a higher supersaturation at both the beginning of the batch and the end of the batch.

For  $j$  is not equal to one, different  $j$  values primarily affect the optimal trajectory at the beginning of the batch. Higher powers of the moment term in Equation 49 cause a lower total nucleation rate. Mathematically, the reason is that the numerical value of the third moment is less than one. Therefore for same level of supersaturation and same value of the third moment, the nucleation rate for higher  $j$  value is lower. Again, since the power of the moment is not zero, higher third moment of the crystal will cause higher nucleation rate. During the batch, the third moment is always increasing. Therefore for  $j$  equal to one, two and three, having higher supersaturation at the beginning of the batch is better than at the middle of the batch. Moreover, since for same level of supersaturation and same

value of the third moment, the nucleation rate for higher  $j$  value is less, the system with higher  $j$  values can tolerate higher supersaturation compared to systems with smaller  $j$ . Therefore, for higher  $j$  value system, the optimal trajectory tends to have a higher supersaturation at the beginning of the batch compared to lower  $j$  value systems.

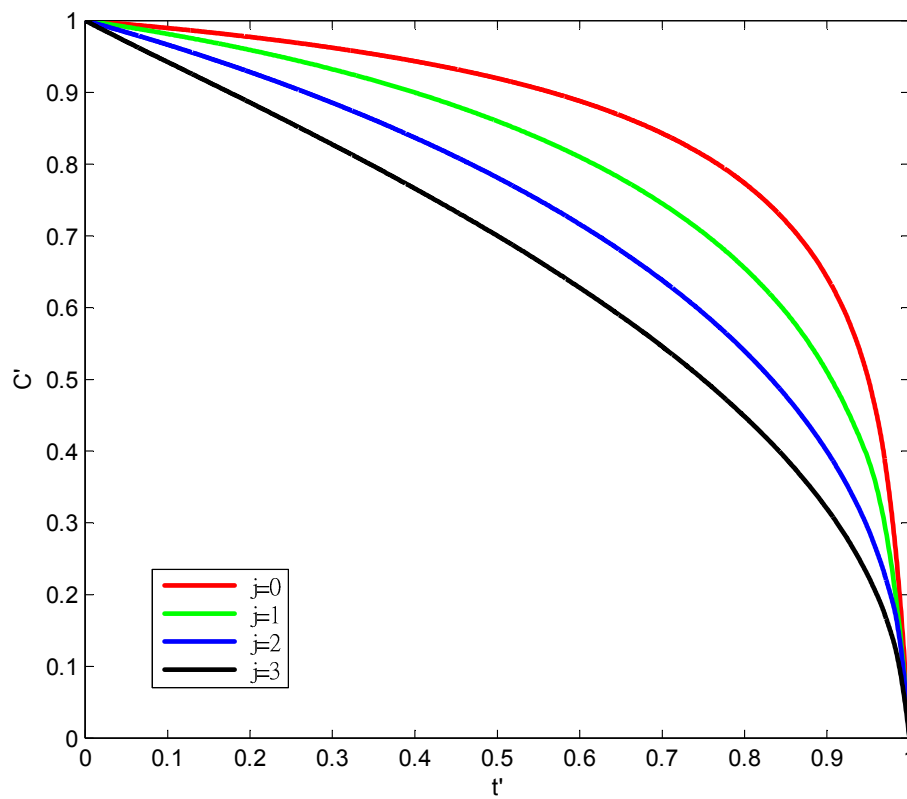


**Figure 35:** The concentration trajectory for different  $j$  value.

Figure 35 shows the dimensionless concentration trajectory during the batch. Because of the definition, the dimensionless concentration decreases from one to zero during the batch. The dimensionless concentration trajectory

when  $j=3$  decreases more evenly during the batch than the others. Since amount of the solute in the solution is consumed by crystal nucleation and crystal growth, and both of them is higher for higher  $j$  system, the solute in higher  $j$  system is consumed faster. Therefore, the dimensionless concentration trajectory for higher  $j$  value is decreasing faster.

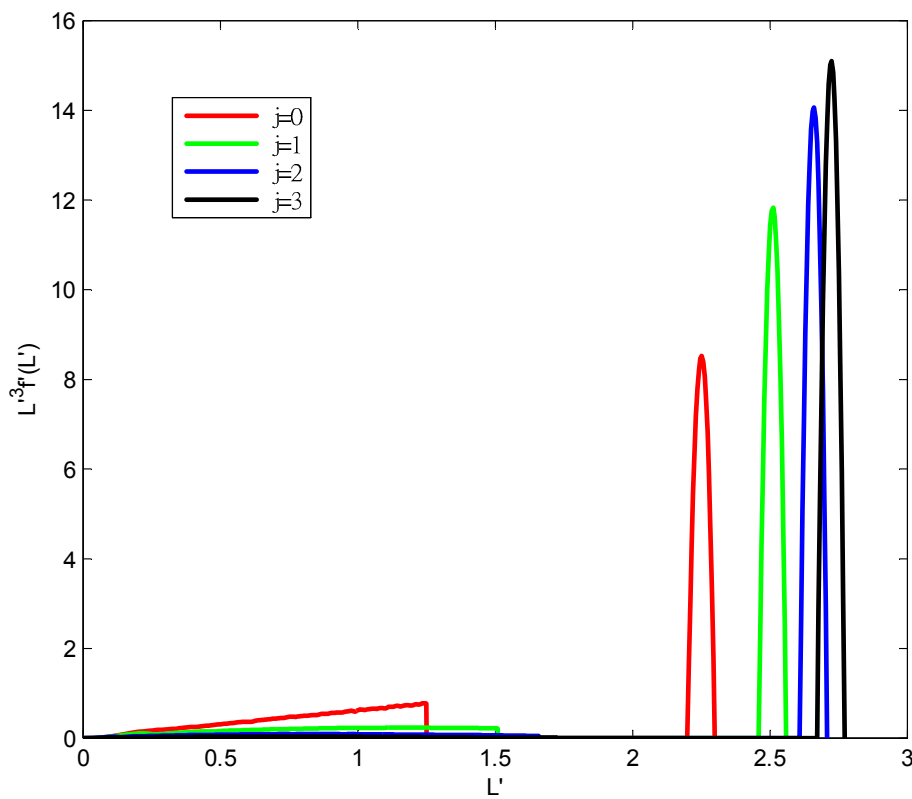


**Figure 36:** Final crystal size distribution for different  $j$  value.

Figure 36 shows the weigh base final crystal size distribution. The area under each curve is proportional to mass of the crystal. There are two peaks in this figure for each  $j$  value. The peak closer to  $L'=0$  represents the nucleated

crystals, and the other parabolic peaks represent the seed crystals. The objective function is to minimize the nucleated crystal mass, and the optimal result is better when  $j$  is larger. This is because the numerical value of the third moment is less than one, therefore for higher power on the moment term in Equation 49, the nucleation rate is actually less, which causes the suppression of the mass of nucleated crystals.

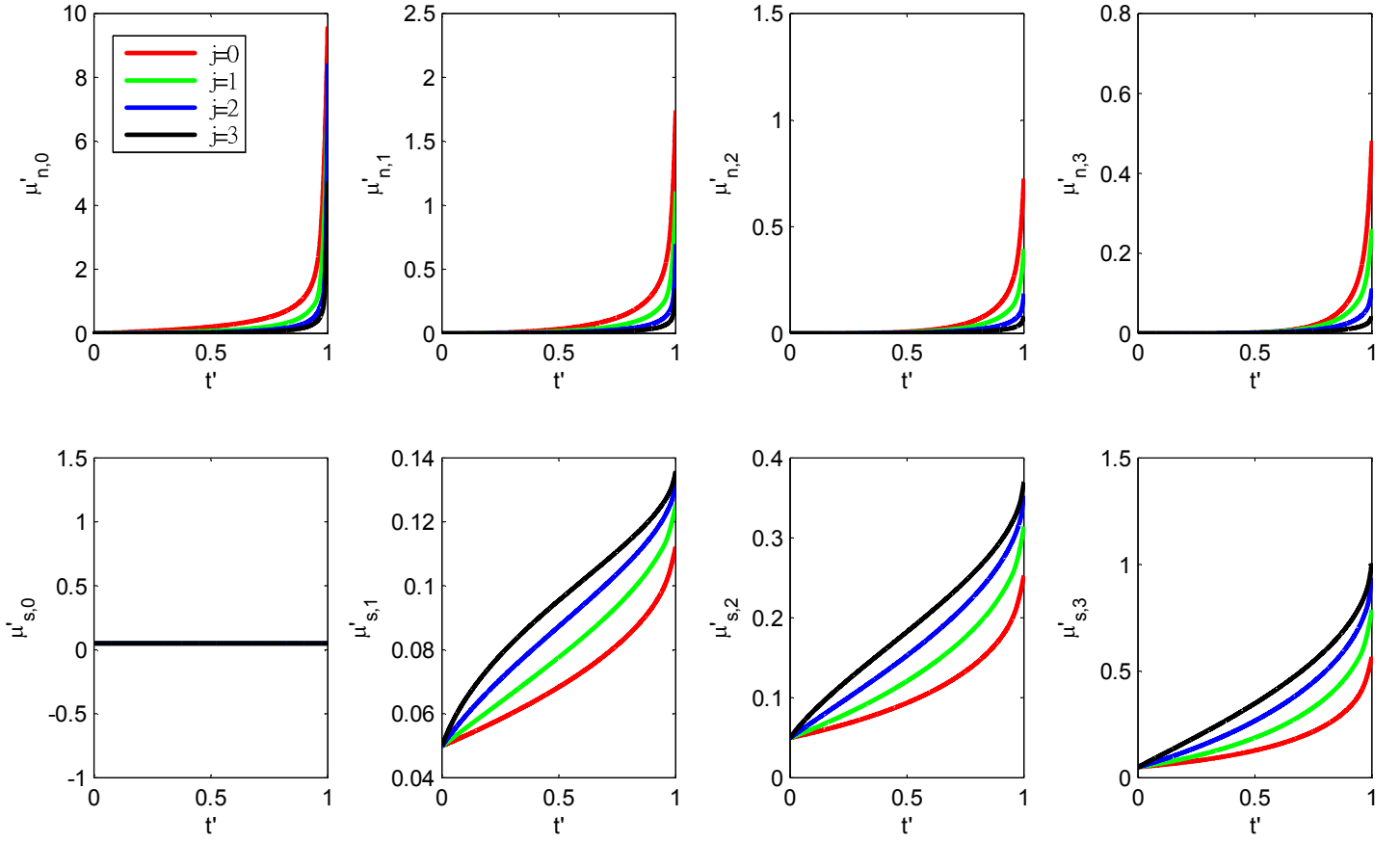


**Figure 37:** Different moment during the batch for different  $j$  value.

## 5. Conclusion

We collected objective functions that researchers have used for optimizing the batch crystallizers, and we optimized the growth trajectory with all of these different objective functions. The result shows that the optimal trajectory for each objective function can be determined. However, some objective functions cause excess nucleation. For seeded batch crystallization, the goal is to grow the seeds while minimizing nucleation. When optimizing with the objective function “minimizing the crystal weight coefficient of variation”, a narrow distributed crystal is achieved by growing a narrow distribution of nuclei so that there is excess nucleation at the beginning of the batch. This is undesirable for a seeded batch crystallizer. Therefore, for each objective function, we also determine the value of the objective function after the nucleated crystals are removed.

We compare the objective function after the nucleated crystals are removed and found out that no matter what objective function we used to evaluate the result, the result that is optimized from objective function “minimizing the third moment of the nucleated mass ( $\mu'_{3n}$ )” always shows a better value. Therefore we conclude that in almost all instances the most

appropriate objective function is minimizing the third moment of the nucleated mass,  $\mu'_{3n}$ .

For objective function that minimizes the weight coefficient of variation we also tried optimizing it by changing seed properties. We found that it is more efficient to achieve a narrow final crystal size distribution by changing seed properties than changing growth trajectory. Large seed loading and narrow seed distribution can prevent excess nucleation when optimize the growth trajectory using objective function “minimizing weight coefficient of variation.”

The system with different value of the exponent on third moment in the nucleation rate equation is also investigated. Nucleation is reduced in system with higher  $j$  value. When optimize with objective function “minimizing the third moment of the nucleated mass,” systems with higher  $j$  value achieve better result. As  $j$  increases, it is also desirable to use a higher growth rate at the beginning of the batch.

## 6. Notations

- B nucleation rate ( $\#/(m^3 s)$ )
- C concentration (mass of dissolved solute per unit volume of suspension) ( $kg/m^3$ )
- $C_0$  initial batch concentration
- $C_f$  final batch concentration
- f crystal size distribution function ( $\#/m^3 m$ )
- G crystal growth rate (m/s)
- g growth parameter (dimensionless)
- $k_b$  nucleation parameter ( $1/(m^3 s)(m/s)^{-\gamma}$ )
- $k_g$  growth parameter (m/s)( $kg/m^3$ ) $^{-g}$
- $k_v$  volumetric shape factor (dimensionless)
- L crystal size (length) (m)
- $m_s$  mass of seeds per unit volume of suspension ( $kg/m^3$ )
- $n_0$  number of seeds per unit volume of suspension ( $\#/m^3$ )
- S supersaturation ( $kg/m^3$ )
- t time (s)
- $t_f$  final batch time (batch duration) (s)
- $x_0$  initial seed size (length) (m)
- w width of parabolic seed distribution (m)



$\gamma$  nucleation parameter (dimensionless)

$j$  nucleation parameter (dimensionless)

$\mu_i$   $i$ th moment of the crystal size distribution ( $m^i/m^3$ )

$\mu_{si}$   $i$ th moment of seed-grown crystal size distribution ( $m^i/m^3$ )

$\mu_{ni}$   $i$ th moment of nucleated crystal size distribution ( $m^i/m^3$ )

$\rho$  crystal density ( $kg/m^3$ )



## 7. Reference

- 1 Jones AG, Crystallization Process Systems, Butterworth-Heinemann: Oxford, 2002.
- 2 Jones AG. Optimal operation of a batch cooling crystallizer. Chem Eng Sci. 1974;29:1075–1087.
- 3 Kubota N, Doki N, Yokota M, Sato A. Seeding policy in batch cooling crystallization. Powder Technology 2001;121(1): 31-38.
- 4 Lung-Somarriba BLM, Moscosa-Santillan M, Porte C, Delacroix A. Effect of seeded surface area on crystal size distribution in glycine batch cooling crystallization: a seeding methodology. Journal of Crystal Growth 2004;270(3-4): 624-32.
- 5 Hojjati H, Rohani S. Cooling and seeding effect on supersaturation and final crystal size distribution (CSD) of ammonium sulphate in a batch crystallizer. Chemical Engineering and Processing 2005;44(9): 949-57.
- 6 Chung SH, Ma DL, Braatz RD. Optimal seeding in batch crystallization. Can J Chem Eng. 1999; 77: 590–596.
- 7 Mullin JW, Nyvlt J. Programmed Cooling of Batch Crystallizers. Chemical Engineering Science 1971;26(3): 369-377.

- 8 Choong, K. L. and R. Smith . Optimization of batch cooling crystallization. Chemical Engineering Science 2004;59(2): 313-327.
- 9 J. D. Ward, C. C. Yu, et al. A New Framework and a Simpler Method for the Development of Batch Crystallization Recipes. Aiche Journal 2011;57(3): 606-617.
- 10 J. D. Ward, D. A. Mellichamp, and M. F. Doherty, Choosing an operating policy for seeded batch crystallization, AIChE J. 52, 2046-2054 (2006). (SCI, EI)
- 11 Rawlings JB, Miller SM, Witkowski WR. Model identification and control of solution crystallization processes: A Review. Ind Eng Chem Res. 1993; 32: 1275–1296.
- 12 Chang CT, Epstein MAF. Identification of Batch Crystallization Control Strategies Using Characteristic Curves. In: Nucleation, Growth and Impurity Effects in Crystallization Process Engineering; EpsteinMAF, ed. AIChE: New York; 1982.
- 13 Eaton JW, Rawlings JB. Feedback control of chemical processes using on-line optimization techniques. Comput Chem Eng. 1990; 14: 469–479.
- 14 Jones AG. Optimal operation of a batch cooling crystallizer. Chem Eng Sci. 1974; 29: 1075–1087.

- 15 Ma DL, Braatz RD. Robust identification and control of batch processes. *Comput Chem Eng.* 2003; 27: 1175–1184.
- 16 Choong KL, Smith R. Optimization of batch cooling crystallization. *Chem Eng Sci.* 2004; 59: 313–327.
- 17 Nagy, Z. K. Model based robust control approach for batch crystallization product design. *Computers & Chemical Engineering* 2009; 33(10): 1685-1691.
- 18 Sheikhzadeh, M., M. Trifkovic, et al. Real-time optimal control of an anti-solvent isothermal semi-batch crystallization process. *Chemical Engineering Science* 2008; 63(3): 829-839.
- 19 Trifkovic, M., M. Sheikhzadeh, et al. Kinetics estimation and single and multi-objective optimization of a seeded, anti-solvent, isothermal batch crystallizer. *Industrial & Engineering Chemistry Research* 2008; 47(5): 1586-1595.
- 20 Paengjuntuek, W., P. Kittisupakom, et al. Optimization and nonlinear control of a batch crystallization process. *Journal of the Chinese Institute of Chemical Engineers* 2008; 39(3): 249-256.

- 21 Nagy, Z. K., J. W. Chew, et al. Comparative performance of concentration and temperature controlled batch crystallizations. *Journal of Process Control* 2008; 18(3-4): 399-407.
- 22 Yang, A. D., G. Montague, et al. Importance of heterogeneous energy dissipation in the modeling and optimization of batch cooling crystallization. *Industrial & Engineering Chemistry Research* 2007; 46(22): 7177-7187.
- 23 Elsner, M. P., G. Ziornek, et al. Simultaneous preferential crystallization in a coupled, batch operation mode - Part 1: Theoretical analysis and optimization. *Chemical Engineering Science* 2007; 62(17): 4760-4769.
- 24 Sarkar, D., S. Rohani, et al. Multi-objective optimization of seeded batch crystallization processes. *Chemical Engineering Science* 2006; 61(16): 5282-5295.
- 25 Costa, C. B. B., A. C. da Costa, et al. Mathematical modeling and optimal control strategy development for an adipic acid crystallization process. *Chemical Engineering and Processing* 2005; 44(7): 737-753.
- 26 Worlitschek, J. and M. Mazzotti Model-based optimization of particle size distribution in batch-cooling crystallization of paracetamol. *Crystal Growth & Design* 2004; 4(5): 891-903.

- 27 Choong, K. L. and R. Smith. Novel strategies for optimization of batch, semi-batch and heating/cooling evaporative crystallization. Chemical Engineering Science 2004; 59(2): 329-343.
- 28 Choong, K. L. and R. Smith. Optimization of batch cooling crystallization. Chemical Engineering Science 2004; 59(2): 313-327.
- 29 Choong, K. L. and R. Smith. Optimization of semi-batch reactive crystallization processes. Chemical Engineering Science 2004; 59(7): 1529-1540.
- 30 Nagy, Z. K. and R. D. Braatz. Robust nonlinear model predictive control of batch processes. Aiche Journal 2003; 49(7): 1776-1786.
- 31 Nagy, Z. K. and R. D. Braatz. Worst-case and distributional robustness analysis of finite-time control trajectories for nonlinear distributed parameter systems. Ieee Transactions on Control Systems Technology 2003; 11(5): 694-704.
- 32 Ma, D. L., S. H. Chung, et al. Worst-case performance analysis of optimal batch control trajectories. Aiche Journal 1999; 45(7): 1469-1476.